The Plant Cell, Vol. 15, 2058–2075, September 2003, www.plantcell.org © 2003 American Society of Plant Biologists

Involvement of the Secretory Pathway and the Cytoskeleton in Intracellular Targeting and Tubule Assembly of *Grapevine fanleaf virus* Movement Protein in Tobacco BY-2 Cells

Céline Laporte,[a] Guillaume Vetter,[a] Anne-Marie Loudes,[a] David G. Robinson,[b] Stefan Hillmer,[b] Christiane Stussi-Garaud,[a] and Christophe Ritzenthaler[a,1]

[a] Institut de Biologie Moléculaire des Plantes, 67084 Strasbourg Cedex, France

[b] Department of Cell Biology, Heidelberg Institute for Plant Sciences, University of Heidelberg, D-69120 Heidelberg, Germany

Grapevine fanleaf virus **(GFLV) is one of a large class of plant viruses whose cell-to-cell transport involves the passage of virions through tubules composed of virus-encoded movement protein (MP). The tubules are embedded within modified plasmodesmata, but the mechanism of targeting of MP to these sites is unknown. To study intracellular GFLV MP trafficking, a green fluorescent protein–MP fusion (GFP:MP) was expressed in transgenic tobacco BY-2 suspension cells under the control of an inducible promoter. We show that GFP:MP is targeted preferentially to calreticulin-labeled foci within the youngest cross walls, where it assembles into tubules. During cell division, GFP:MP colocalizes in the cell plate with KNOLLE, a cytokinesis-specific syntaxin, and both proteins are linked physically, as shown by coimmunoprecipitation of the two proteins from the same microsomal fraction. In addition, treatment with various drugs has revealed that a functional secretory pathway, but not the cytoskeleton, is required for tubule formation. However, correct GFP:MP targeting to calreticulin-labeled foci seems to be cytoskeleton dependent. Finally, biochemical analyses have revealed that at least a fraction of the MP behaves as an intrinsic membrane protein. These findings support a model in which GFP:MP would be transported to specific sites via Golgi-derived vesicles along two different pathways: a microtubule-dependent pathway in normal cells and a microfilament-dependent default pathway when microtubules are depolymerized.**

INTRODUCTION

The endomembrane system and the cytoskeleton cooperate in numerous intracellular transport processes in both normal and pathological conditions. In plants, there is evidence that these structures play a pivotal role in viral infection. Viral invasion of a plant is a complex process that requires the sequential accomplishment of key events such as viral genome replication, cell-to-cell movement, and long-distance transport. Cell-to-cell viral movement is mediated by so-called viral movement proteins (MPs) and occurs through plasmodesmata, small pores in the cell wall that establish cytoplasmic, plasma membrane, and endoplasmic reticulum (ER) continuity between adjacent cells (McLean et al., 1997; Ehlers and Kollmann, 2001). Previous studies have identified two major classes of MP. The first class, of which *Tobacco mosaic virus* (TMV) 30-kD MP is the best studied example, involves a single MP assumed to function as a molecular chaperone that binds viral RNA and transports it to plasmodesmata. There, the MP presumably acts to increase the size exclusion limit of the plasmodesmata and to facilitate the movement of the viral RNA/MP complex into neighboring uninfected cells (for review, see Heinlein, 2002). In the second class, exemplified by *Cowpea mosaic virus* (CPMV), movement differs from the TMV paradigm in that both MP and the virions are required for cell-to-cell transport. In this case, movement is thought to occur through tubules embedded within highly modified plasmodesmata that transport intact virions rather than viral RNA (Lazarowitz and Beachy, 1999). Using different technical approaches, the MP has been identified as a major structural component of these tubules (Lazarowitz and Beachy, 1999).

More recently, attention has turned to the question of how intracellular transport and targeting of MP to plasmodesmata occur. Pioneering work with TMV MP has demonstrated a close association of the MP with elements of the cytoskeleton such as microtubules and microfilaments (Heinlein et al., 1995; McLean et al., 1995) as well as with the ER (Heinlein et al., 1998). A model for TMV movement has been presented in which the MP transports viral RNA along the cytoskeleton to the desmotubule, the appressed domain of the ER that constitutes the central component of plasmodesmata (Mas and Beachy, 1999). However, the exact roles of the TMV MP/microtubule complex in the infection process, and of interactions between MP and the endomembrane system in general, remain a subject of controversy. Using virus derivatives modified to express TMV MP fused to green fluorescent protein (GFP), Boyko and co-workers (Boyko et al., 2000a, 2000b, 2002) demonstrated a strict correlation between the ability of MP variants to associate with microtubules to enable cell-to-cell movement. However, experiments with a "DNA-shuffled" TMV MP mutant showing limited affinity for microtubules led to the hypothesis that the MP–microtubule interaction is involved in a proteasome-dependent MP degradation pathway rather than in viral RNA transport (Reichel and Beachy, 2000; Gillespie et al., 2002).

MP association with the ER also has been reported for viruses whose MPs form tubules. For examples, the *Alfalfa mo-*

[1] To whom correspondence should be addressed. E-mail christophe.ritzenthaler@ibmp-ulp.u-strasbg.fr; fax 33-388-614-442.

Article, publication date, and citation information can be found at www.plantcell.org/cgi/doi/10.1105/tpc.013896.

saic virus MP behaves as an integral membrane protein and localizes to the ER (Huang and Zhang, 1999). In the case of CPMV and *Cauliflower mosaic virus*, tubule assembly was shown to be independent of microtubules or microfilaments (Huang et al., 2000, 2001; Pouwels et al., 2002) but to require a functional secretory pathway (Huang et al., 2000; Pouwels et al., 2002). Thus, treatment with brefeldin A (BFA), a fungal macrocyclic lactone known to perturb the endomembrane system in plants (Nebenführ et al., 2002; Ritzenthaler et al., 2002b), resulted in the inhibition of tubule formation and the redistribution of the MP to multiple foci present at the periphery of protoplasts (Huang et al., 2000; Pouwels et al., 2002). These foci could represent sites of tubule nucleation, which suggests that BFA interfered not with the targeting of MP but with tubule formation (Huang et al., 2000; Pouwels et al., 2002).

Grapevine fanleaf virus (GFLV), a nepovirus, possesses a bipartite genome and is related closely to CPMV. It also uses a tubule-guided movement mechanism, as demonstrated previously by the capacity of its MP to form tubules containing virus-like particles in GFLV-infected *Chenopodium quinoa* plants and protoplasts (Ritzenthaler et al., 1995b). The GFLV MP (protein 2B) is released from its viral RNA 2–encoded polyprotein precursor by maturation, a process that requires the proteolytic activity of protein 1D encoded by RNA 1 (Margis et al., 1993). GFLV replication induces the formation of a viral "replication compartment" at the periphery of the nucleus, in which numerous ER-derived membranes accumulate to support replication (Gaire et al., 1999; Ritzenthaler et al., 2002a). This replication compartment may be the primary site at which MP is synthesized and matured, because GFLV RNA 2 is strictly dependent on RNA 1 for its replication, and MP release from its polyprotein precursor depends on the 1D protease. Nevertheless, MP does not accumulate significantly in the viral replication compartment (Ritzenthaler et al., 2002a), suggesting that it is transported rapidly by an unknown mechanism to the cell periphery, where tubule assembly occurs.

In this investigation, we have addressed the question of how the MP of GFLV is transported to the cell periphery. For this, we used stably transformed suspension-cultured tobacco BY-2 cells expressing a GFP:MP fusion under the control of an inducible promoter. We show that in these cells the GFP:MP fusion protein forms tubules similar to those observed in infected plant tissue and protoplasts. Confocal laser scanning microscopy (CLSM) and transmission electron microscopy were used to examine the spatial distribution of the tubules in relation to components of the plasmodesmata and the cell plate. Specific drugs were used to analyze the roles of the cytoskeleton and the endomembrane system in GFP:MP targeting and tubule assembly. Finally, the association of the MP with membranes and marker proteins was studied using biochemical approaches.

RESULTS

Tight Control of GFP:MP Gene Expression Can Be Accomplished in BY-2 Cells

A construct containing the GFP sequence fused to the N terminus of the GFLV 2B MP sequence was generated, with the sequence encoding the GFP:MP fusion under the control of the pUAS-Gal4 glucocorticoid-inducible promoter (Aoyama and Chua, 1997). This plasmid (pTA7002-GFP:MP) was used for *Agrobacterium tumefaciens*–mediated transformation of tobacco BY-2 cells. After selection with hygromycin, individual calli were monitored for GFP:MP expression by epifluorescence microscopy after induction with dexamethasone. Line 2B15, which expressed high levels of GFP:MP after induction, was selected and maintained in liquid BY-2 medium under standard conditions.

The accumulation of GFP:MP in the 2B15 cell line was tested by protein gel blot analysis using MP-specific antibodies. No signal was detected in total protein extracts from wild-type BY-2 cells treated with dexamethasone (Figure 1, lane C). Before the addition of dexamethasone, only a very faint band of ~68 kD (the calculated molecular mass of GFP:MP), which might correspond to the leaky expression of GFP:MP, was visible in the extract from the 2B15 cell line (Figure 1, lane 1). A 68-kD band became clearly visible 2 h after induction, and its intensity increased up to 24 h after induction (Figure 1, lanes 2 to 8). Additional bands of lower molecular mass, probably corresponding to GFP:MP degradation products or translational intermediates, also were detected after induction. These results confirm the previously described high specificity of the MP antibodies toward GFP:MP (Ritzenthaler et al., 1995a) and also indicate that tight control of GFP:MP expression can be achieved in transgenic BY-2 cells using the glucocorticoid induction system.

GFP:MP Is Targeted to Plasmodesmata and Assembles into Fluorescent Threads

When observed by CLSM, no fluorescence was detected in noninduced 2B15 cells (data not shown). By contrast, discrete punctate light sources dispersed throughout the cytoplasm and within cross walls became visible 9 to 10 h after induction in

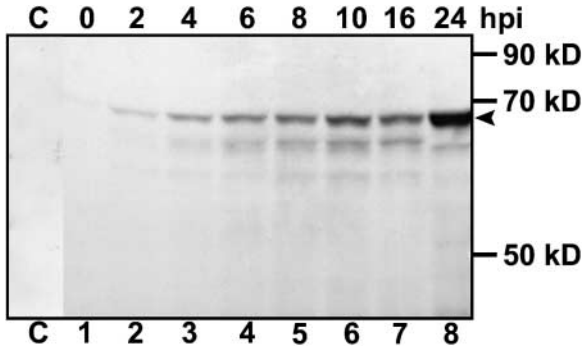

Figure 1. Kinetics of GFP:MP Induction with Dexamethasone in 2B15 Cells.

Total proteins from wild-type cells 24 h after induction (lane C), noninduced 2B15 cells (lane 1), and induced 2B15 cells (lanes 2 to 8) were examined by immunoblot analysis using affinity-purified anti-MP immunoglobulins. Induction times were 0, 2, 4, 6, 8, 10, 16, and 24 h (hpi; lanes 1 to 8, respectively). The arrowhead indicates the position of GFP:MP on the gel. Molecular mass markers are indicated at right.

dexamethasone-treated 2B15 cells (data not shown). By 24 h after induction, the cytoplasmic fluorescent punctate bodies remained unchanged in form (Figure 2A, arrows), whereas the discrete fluorescence associated with cross walls (generally one of two cross walls, as discussed below) appeared as thin thread-like structures of variable length (often several micrometers; Figure 2A, arrowheads). Such structures never were observed in transformed BY-2 cells expressing GFP alone (data not shown). Combining the fluorescence and differential interference contrast images of the same cell (Figure 2B) revealed that the fluorescent threads protruded from the cross walls that separate adjacent cells into the cytosol of neighboring cells (BY-2 daughter cells often do not separate after mitosis/cytokinesis and hence form linear chains in which the walls that separate adjacent cells can be referred to as "cross walls"). Threads never were observed at side walls, suggesting that they may be associated with plasmodesmata, which are present exclusively in cross walls. At higher magnifications, the thread-like structures clearly were oriented and extended from the cross wall into the cytosol of one or the other neighboring cell, and never from the cytosol of one cell through the cross wall into the cytoplasm of the neighboring cell (Figure 2C).

To exclude the possibility that the formation of the thread-like structures was specific to BY-2 cells or suspension-cultured cells in general, *Nicotiana benthamiana* leaves were agroinfiltrated for transient GFP:MP expression and observed 24 h after induction by CLSM. In epidermal cells, most of the fluorescence was concentrated in thread-like structures protruding from the walls (Figures 2D and 2E). As in BY-2 cells, punctate fluorescence also was observed within the cytosol of transfected cells. Because no significant difference was detected in the capacity of *N. benthamiana* and BY-2 cells to form GFP:MP threads, our studies were continued on 2B15 cells because of their controlled manipulability.

To further study the possible association of the GFP:MP fluorescent threads with plasmodesmata, cells were subjected to plasmolysis 24 h after induction. As reported originally by Hecht (1912), plasmolysis leads to the formation of thin membranous structures known as Hechtian strands that anchor the plasma membrane to the cell wall. More recently, CLSM has been used to demonstrate that, in cross walls, many Hechtian strands originate at or close to the entrances of plasmodesmata (Pont-Lezica et al., 1993; Oparka et al., 1994). As expected, numerous Hechtian strands (Figures 2G and 2H, double arrowheads) arose from both cross walls and side walls upon plasmolysis of induced 2B15 cells, as seen by differential interference contrast imaging (Figures 2F to 2H). Most of the fluorescent threads remained attached to the cross walls when the protoplast retracted (Figures 2G and 2H). On some occasions, however, plasmolysis resulted in breakage of the fluorescent threads, probably as a result of excessive longitudinal tension (Figure 2G, open arrowhead). When plasmolysis was sufficient to generate Hechtian strands longer than the fluorescent threads, it became evident that essentially all of the fluorescent threads attached to the cross walls were embedded within Hechtian strands, also demonstrating that threads are formed within and not outside of the cell protoplast (Figure 2H).

Because most Hechtian strands present within cross walls are intimately linked to plasmodesmata (Oparka et al., 1994), and bearing in mind that calreticulin is a known marker for plasmodesmata (Baluška et al., 1999), further experiments were performed to test the possible association of the green fluorescent threads with plasmodesmata. As observed previously in maize cells (Baluška et al., 1999), calreticulin antibodies (red) labeled punctate structures in cross walls (Figures 2I and 2J, open arrows). The great majority of the green fluorescent threads were seen to extend from calreticulin-labeled spots, although not all of the calreticulin-labeled spots were associated with fluorescent threads (Figures 2I and 2J, asterisks). In the absence of primary antibodies, no labeling was observed (Figure 2K). Therefore, we conclude that the GFP:MP fluorescent threads form within cross walls at specific calreticulin-labeled foci related to Hechtian attachment sites and possibly also to plasmodesmata.

Fluorescent Threads Correspond to GFP:MP Tubules

To gain a direct insight into the ultrastructure of the fluorescent threads and their possible relationship to plasmodesmata, noninduced and induced cells were fixed and processed for transmission electron microscopy. In noninduced 2B15 cells, typical primary plasmodesmata were visible in cross walls (Figure 3A, arrows), whereas in cells at 24 h after induction, tubule-like structures frequently were detected within cross walls (Figures 3B to 3D). Cell wall protrusions often surrounded the base of the tubules (Figures 3B and 3C). The outer surface of these tubules was clearly lined with plasma membrane, as seen in longitudinal sections (Figure 3C, black arrowhead), demonstrating cytosolic continuity between neighboring 2B15 cells. In cross-section, tubules measured ~78 nm in diameter, and their central cavity was filled with electron-dense material that appeared structured (Figure 3D, white arrowhead). In contrast to normal plasmodesmata (Figure 3A, arrows), no desmotubule or ER connections were observed within the tubules (Figures 3C and 3D).

As in the case of the fluorescent threads observed by CLSM, the tubules in thin sections always extended from the cell wall toward the cytoplasm. To confirm their coidentity with the fluorescent threads observed by CLSM, immunogold labeling was performed. Using GFP antibodies, specific gold labeling was observed along the tubules (Figure 3E, white arrows). Affinity-purified MP-specific antibodies, used previously to label MP tubules in GFLV-infected tissues or protoplasts (Ritzenthaler et al., 1995b), proved to be inefficient for decorating GFP:MP tubules by either immunogold or immunofluorescence technique (data not shown). Therefore, we assume that tubule assembly from GFP:MP (but not from MP alone) results in the exposure of the GFP moiety at the outer surface of the tubules, thereby masking the MP epitopes.

In conclusion, our results clearly demonstrate that the GFP:MP protein can form tubules when expressed in BY-2 cells; therefore, it is the only viral protein required for tubule assembly. These tubules always are embedded in cross walls, possibly within highly modified plasmodesmata, and closely resemble the tubular structures observed in GFLV-infected leaf tissue, except for the presence of virus particles in the latter (Ritzenthaler et al., 1995b).

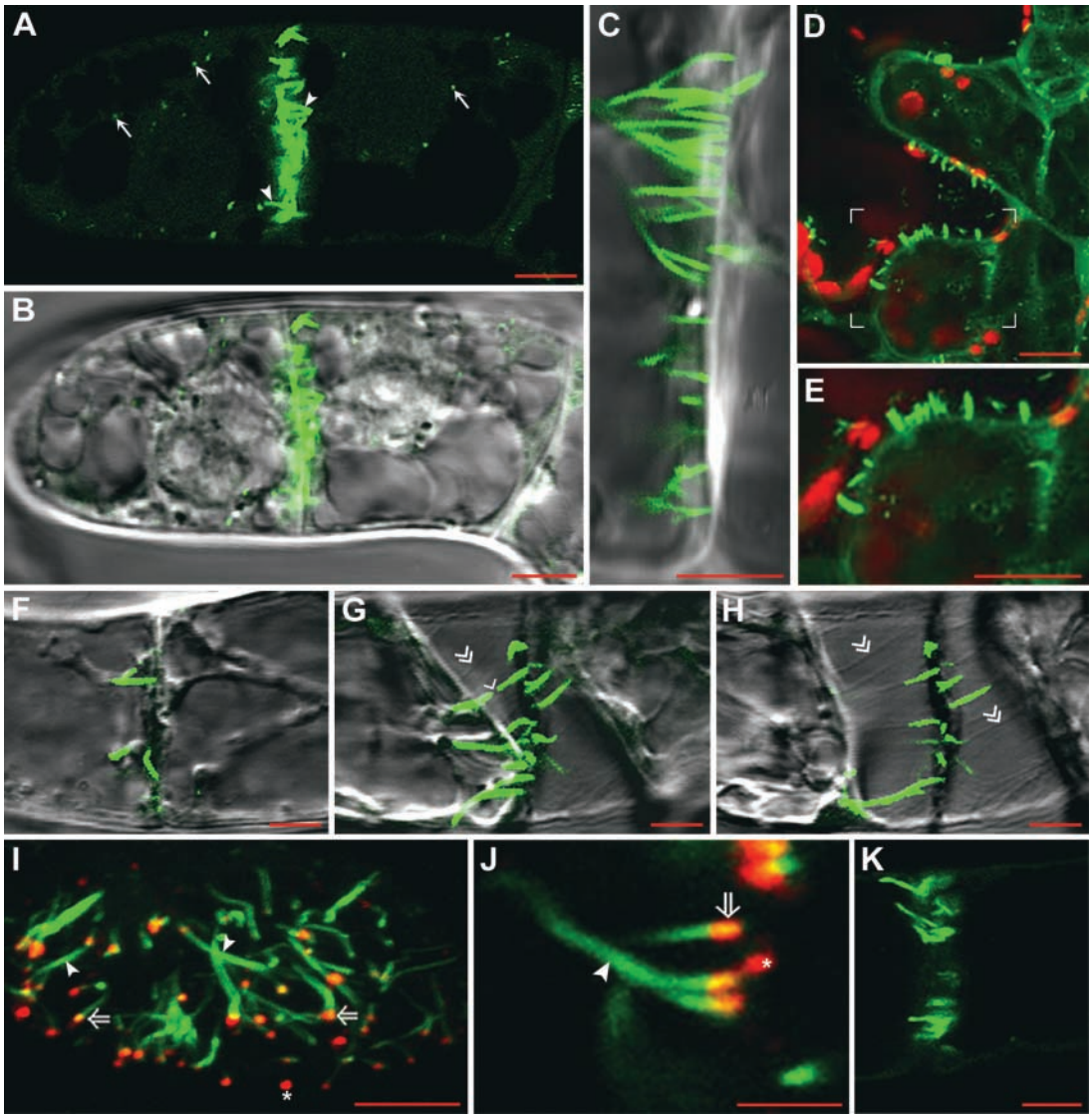

Figure 2. CLSM Analysis of 2B15 Cells 24 h after Induction.

(A) to **(C)** Localization of GFP:MP in living cells.
(A) Bright fluorescent thread-like structures (arrowheads) are visible in cross walls. Fluorescent punctate bodies are observed in the cytoplasm (arrows).
(B) Composite image between **(A)** and a differential interference contrast (DIC) image.
(C) Detailed view of a cross wall from which numerous oriented fluorescent thread-like structures arise (GFP:MP channel and DIC image merged).
(D) and **(E)** Localization of GFP:MP in *N. benthamiana* leaf cells. Leaves were induced 3 days after agroinfiltration and observed 24 h after induction.
(D) Fluorescent threads are observed in walls between two epidermal cells. Chloroplasts are shown in red.
(E) Details of the boxed region shown in **(D)**.
(F) to **(H)** Behavior of the fluorescent thread-like structures during plasmolysis. Mannitol (0.45 M) was added and plasmolysis was followed with the microscope as a function of time before the addition of mannitol **(F)**, at 4.5 min of plasmolysis **(G)**, and at 10 min of plasmolysis **(H)**. Hechtian strands that connect the retracting protoplast plasma membrane to the cell wall are visible (double arrowheads). Fluorescent threads are present within Hechtian strands and remain attached to the cell wall during plasmolysis. Excessive tension provoked the breakage of some tubules during plasmolysis (single arrowhead). The GFP:MP channel and the DIC image are merged in all images.
(I) to **(K)** Calreticulin immunolocalization in GFP:MP-expressing cells. Induced cells containing green fluorescent threads (arrowheads) were fixed and labeled with calreticulin antibodies (red signals). The GFP:MP and calreticulin-specific channels are merged in the images.
(I) The cells were oriented so that the cross wall appears in face view.
(J) Side view of a cross wall at higher magnification.
Asterisks indicate typical calreticulin-labeled punctate structures in the cross walls. Fluorescent threads emerge from the calreticulin-labeled foci, as judged by the presence of yellow spots in the merged images (open arrows).
(K) Control induced cell in which the anti-calreticulin antibody was omitted.
(D), **(E)**, and **(I)** represent projections of 19, 19, and 23 optical 0.45-μm sections, respectively. All other images represent single 0.45-μm optical sections. Bars = 5 μm except in **(D)** and **(E)** (10 μm) and **(J)** (2 μm).

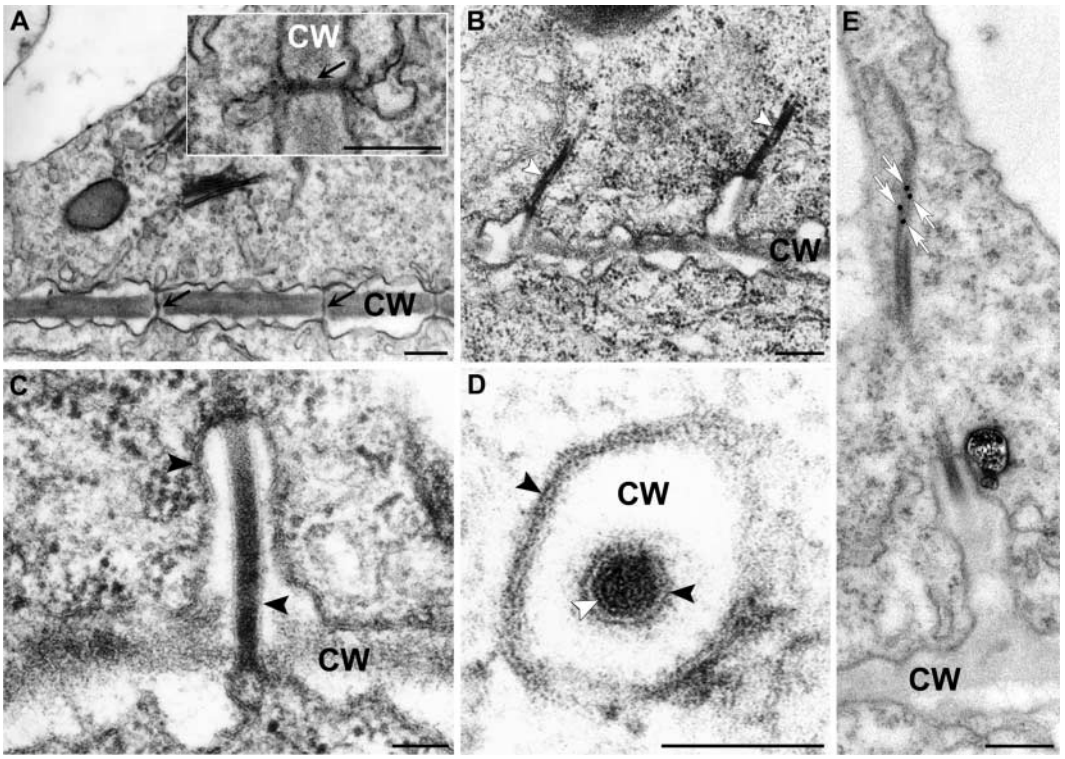

Figure 3. Transmission Electron Microscopy Images of Plasmodesmata and GFP:MP Tubules in Cross Walls of 2B15 Cells Before and 24 h after Induction with Dexamethasone.

(A) Before induction. Normal plasmodesmata (arrows) are visible in cross walls from noninduced cells. The inset shows a higher magnification view of a plasmodesma in the horizontal orientation.

(B) to **(E)** Twenty-four hours after induction.

(B) Oriented tubules associated with cross walls from induced cells (white arrowheads). Note the electrolucent cell wall protrusions surrounding the basal part of the tubules.

(C) and **(D)** Detailed view of a tubule in longitudinal section **(C)** and in cross-section **(D)**. Note the electron-dense material that fills the central cavity (white arrowhead) and the plasma membrane lining the exterior of the tubules (black arrowheads).

(E) Immunogold labeling (10-nm gold particles) of a tubule with GFP-specific antiserum. The white arrows indicate gold beads.

Bars = 500 nm except in **(A)** inset, **(C)**, and **(D)** (200 nm).

GFP:MP Is Targeted Preferentially to the Cell Plate, but Cytokinesis Is Not Required for Tubule Formation

As mentioned in our initial description of the 2B15 cells (see above), we observed that tubules assembled preferentially in one of two cross walls within the polar cell chains formed by BY-2 cells (Figures 2B and 4A). As a general rule, the cross walls in odd positions from the extremities of these chains were far more enriched in tubules than those in even positions (Figure 4A, arrowheads). Considering that mitosis/cytokinesis frequently occurs synchronously in all of the cells of a chain (data not shown), it was concluded that tubules assembled preferentially in the youngest cross walls (those in odd positions) rather than in the older ones (those in even positions). This observation suggests that efficient tubule formation within the cross walls could be cytokinesis dependent (i.e., that initiation of tubule formation occurs preferentially during phragmoplast maturation and less frequently in preexisting cell walls).

To test this hypothesis, cells were pretreated with 10 mM caffeine for 24 h and then induced for 24 h with dexamethasone in the continued presence of caffeine before CLSM observation. Caffeine is known to inhibit cell plate maturation by specifically disrupting the conversion of the fusion tube–generated network into the tubulovesicular network (Samuels and Staehelin, 1996). In addition, because caffeine leads to the disintegration of the incomplete cell plate without interfering with cell cycle progression (Samuels and Staehelin, 1996; Valster and Hepler, 1997), two types of cells were observed: normal cells (cells that had not divided during treatment) and binucleate cells that arose as a consequence of the aborted cell division process. In normal cells (as judged by the presence of one nucleus per cell), fluorescent tubules still formed preferentially in the youngest cross walls (Figure 4B), thereby excluding cytokinesis as a necessary prerequisite for tubule formation. However, tubules also assembled in cells that underwent cytokinesis during treatment and as a consequence were binucle-

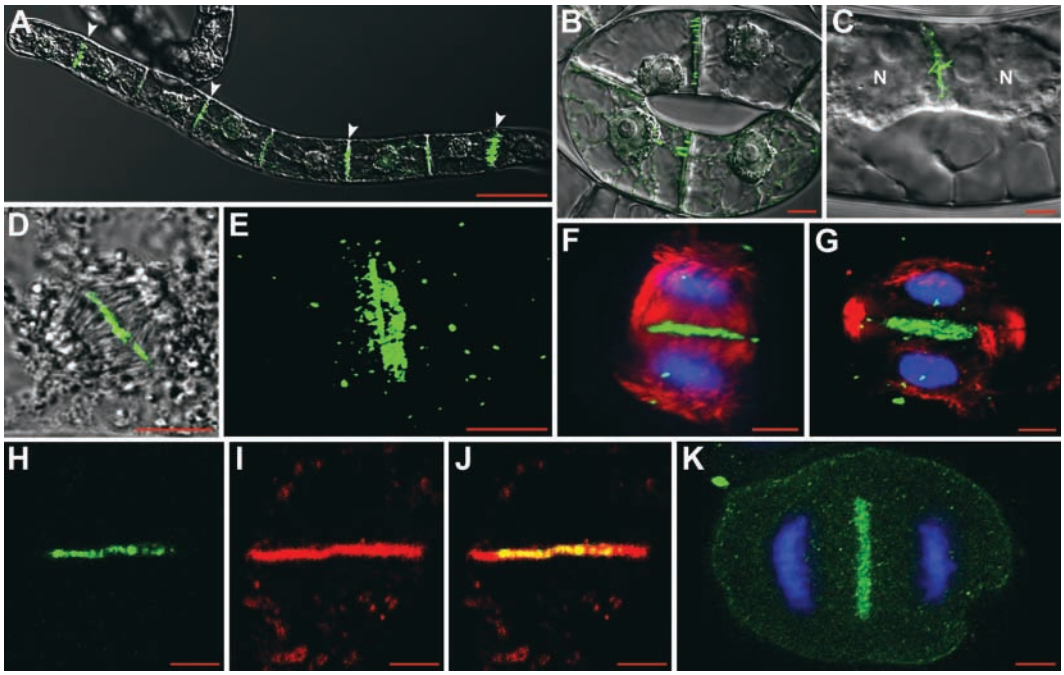

Figure 4. Preferential Targeting of GFP:MP Protein to Young Walls and the Cell Plate.

(A) Tubules assemble preferentially in odd-numbered cross walls from living BY-2 cell chains 24 h after induction (arrowheads).
(B) and **(C)** Tubule formation within caffeine-treated (10 mM) cells 24 h after induction.
(B) Tubules are present within the youngest cross walls in a chain of four cells that have not undergone cell division during the caffeine treatment (mononucleated cells).
(C) Tubules formed exclusively within the aborted plane of division in binucleated cells that have undergone mitosis during caffeine treatment. N, nucleus.
(D) GFP:MP targeting to the cell plate in a BY-2 cell at late anaphase stage, 24 h after induction.
(E) Three-dimensional projection of the cell shown in **(D)**.
(F) and **(G)** Three-dimensional projections showing GFP:MP (green), microtubules (red), and the nuclei after 4′,6-diamidino-2-phenylindole staining (blue) in immunolabeled cells at late anaphase **(F)** and late telophase **(G)**.
(H) to **(J)** GFP:MP and KNOLLE colocalize in the plane of division.
(H) and **(I)** GFP:MP distribution **(H)** and KNOLLE immunolabeling **(I)** in a cell at anaphase stage.
(J) Merged image showing the partial colocalization (yellow signal) of GFP:MP and KNOLLE within the cell plate.
(K) Immunolabeling of the MP in GFLV-infected BY-2 cells at late anaphase stage. The MP (green) accumulates almost exclusively within the cell plate formed between the separated chromosomes (blue).
Single optical sections are shown in **(A)** to **(D)** and **(H)** to **(K)**. **(E)**, **(F)**, and **(G)** show projections of 18, 22, and 44 sections, respectively. All optical sections were 0.45 μm thick. In **(A)** to **(D)**, the GFP:MP channel and differential interference contrast images have been merged. Bars = 5 μm except in **(A)** (50 μm) and **(B)**, **(D)**, and **(E)** (10 μm).

ated (Figure 4C). Remarkably, in these cells, the tubules were not distributed randomly but were formed within the aborted cell plate (Figure 4C), as if GFP:MP and cell plate components trafficked together.

To verify whether GFP:MP is transported similarly to the components of the cell plate, 2B15 cells were monitored during cytokinesis, a process that initiates at late anaphase with the formation of the phragmoplast. During anaphase, GFP:MP accumulated in numerous punctate structures present within the central region of the phragmoplast, which probably corresponds to the plane of division (Figures 4D and 4E). This cell plate–specific localization was confirmed using monoclonal tubulin antibodies that label the phragmoplast microtubules and a KNOLLE antiserum as a marker for the cell plate (Lauber et al., 1997). As seen in Figures 4F and 4G, representing three-dimensional projections of an induced 2B15 cell in late anaphase (Figure 4F) and telophase (Figure 4G) with labeled microtubules (red signal) and chromosomes/nuclei (blue signal), GFP:MP was present almost exclusively within the plane of division. In dividing cells labeled with KNOLLE antibodies, the GFP:MP fluorescence localized with the central portion of the red KNOLLE signal (Figures 4H to 4J), confirming specific GFP:MP accumulation within the cell plate. No signal was obtained in cells when primary antibodies (anti-tubulin or anti-KNOLLE) were omitted (data not shown). Remarkably, MP also immunolocalized within the cell plate of wild-type BY-2 protoplasts infected with GFLV (Figure 4K). This finding formally demonstrates that targeting to the cell plate is an intrinsic property of

the MP and does not depend on the fused GFP moiety. It also establishes the fact that MP targeting to the cell plate occurs in the context of a normal viral infection.

Intracellular Transport of GFP:MP Requires a Functional Secretory Pathway and Is Microtubule Dependent

It is known that phragmoplast-assisted cytokinesis is a dynamic process that involves a complex array of microtubules, actin microfilaments, and different membrane compartments (for review, see Heese et al., 1998; Verma, 2001). To further support the assumption that MP can be transported intracellularly, at least during cytokinesis, together with cell plate components, drugs that specifically affect the endomembrane system or the cytoskeleton were administered to the 2B15 cells during GFP:MP induction.

When applied 8 h after induction (i.e., just before GFP:MP tubules appear in 2B15 cells), BFA (a drug that inhibits COPI vesicle production and leads to the disruption of the Golgi apparatus and the inhibition of the secretory pathway [Nebenführ et al., 2002; Ritzenthaler et al., 2002b]) strongly inhibited tubule formation. In contrast to untreated cells, in which tubules were detected in 72% of the fluorescing cells at 24 h after induction (the remaining 28% of the cells showed diffuse fluorescence together with small punctate cytoplasmic structures [data not shown]), the percentage of cells with tubules decreased to 14% upon addition of BFA (Table 1). In most of the BFA-treated cells, GFP:MP fluorescence was dispersed throughout the cytosol and the nucleus (Figure 5A). As suggested previously (Ritzenthaler et al., 2002b), variability in the sensitivity of cells to BFA probably accounts for the failure of tubules to disappear completely after BFA treatment in a fraction of the fluorescing cells.

Table 1. Effect of Metabolic Inhibitors on Tubule Formation

Inhibitor[a]	Percent of Tubules[b]	Percent of Abnormal Tubules[c]	b/c[d] × 100
None	72	0	0
Latrunculin B (2 μM)	77	0	0
Cytochalasin D (20 μM)	66	0	0
Taxol (2 μM)	65	0	0
Oryzalin (10 μM)	74	35	47
Oryzalin (10 μM)[e]	70	70	100
BFA (10 μg/mL)	14	0	0

[a] Metabolic inhibitors were added 8 h after induction at the indicated final concentrations.
[b] Percentage of fluorescent BY-2 cells that formed tubules. At least 100 fluorescent cells were observed in each case. Unless indicated otherwise, observations were made 24 h after induction (16 h after the addition of inhibitors).
[c] Percentage of fluorescent cells that formed tubules on side walls and cross walls.
[d] b/c relates to percentage of fluorescent BY-2 cells that form tubules (b) divided by the percentage of fluorescent cells that formed tubules on side walls and cross walls (c).
[e] Observed 48 h after induction (40 h after the addition of inhibitors).

On the other hand, treatment of 2B15 cells with cytoskeleton-specific drugs did not interfere with GFP:MP tubule formation. Thus, administration at 8 h after induction with either 2 μM latrunculin or 20 μM cytochalasin D (both of which cause F-actin depolymerization [Coue et al., 1987; Morton et al., 2000]), as verified by the arrest of cytoplasmic streaming and the absence of rhodamine-phalloidin–labeled microfilaments [data not shown]), or 2 μM taxol (a microtubule-stabilizing drug [Weerdenburg et al., 1986; Yasuhara et al., 1993]), as assessed by the presence of numerous multinucleated cells [data not shown]), did not significantly alter the percentage of cells that subsequently supported tubule formation (~70% of the cells; Table 1). Under these conditions, tubules formed preferentially in the youngest cross walls (Table 1).

Interestingly, treatment with oryzalin, an agent known to depolymerize microtubules and to arrest the cell cycle at metaphase (Morejohn et al., 1987; Akashi et al., 1988; Hugdahl and Morejohn, 1993), did not diminish tubule formation significantly (Table 1). However, oryzalin treatment resulted in a highly abnormal intracellular distribution of the GFP:MP tubules. Instead of being localized exclusively at cross walls, as in control cells (Figures 2B and 4A), numerous small fluorescent tubules formed at side walls as well (Figure 5B). The proportion of fluorescent cells that displayed abnormal targeting of the tubules increased with time: ~50% of the tubule-positive cells had tubules at their side walls 16 h after oryzalin addition, increasing to 100% after 40 h of treatment (Table 1).

Plasmolysis experiments demonstrated that neither the side wall nor the cross wall tubules were distributed randomly; rather, they protruded from Hechtian attachment sites. Indeed, during plasmolysis, the tubules did not remain parallel to the protoplast surface as if they were attached to the surface of the retracting plasma membrane but stood erect and were embedded within nascent Hechtian strands (Figures 5C to 5F). In contrast to the cross wall tubules present within the Hechtian strands of untreated 2B15 cells (Figure 2H), those formed after oryzalin treatment always detached from their wall anchorage sites during plasmolysis (Figures 5D to 5F). As expected, no microtubules were visible after oryzalin treatment (Figure 5G).

Surprisingly, the fluorescent tubules that formed on side walls after oryzalin treatment extended from numerous discrete calreticulin antibody–labeled foci present at the cell periphery (Figure 5H), in a manner similar to that observed in cross walls from untreated cells (Figures 2I and 2J). Further observations established that the calreticulin antibodies specifically labeled small punctate structures in both cross walls and side walls of oryzalin-treated and nontreated 2B15 cells (Figure 5I) and also of wild-type BY-2 cells (data not shown), indicating that the labeled foci are normal features of BY-2 cells. Neither the ER network nor any other organelle inside the cells was labeled (Figure 4I).

In agreement with our results obtained after single drug application, complete removal of the cytoskeleton through the simultaneous application of latrunculin and oryzalin had no effect on tubule formation (Figures 5J to 5L). However, a novel distribution of the tubules was observed. Instead of being localized to walls, tubules frequently were found in the cytosol close to the nucleus (Figure 5J), often organized into aster-like structures (Figures 5K and 5L). In these cells, calreticulin labeling

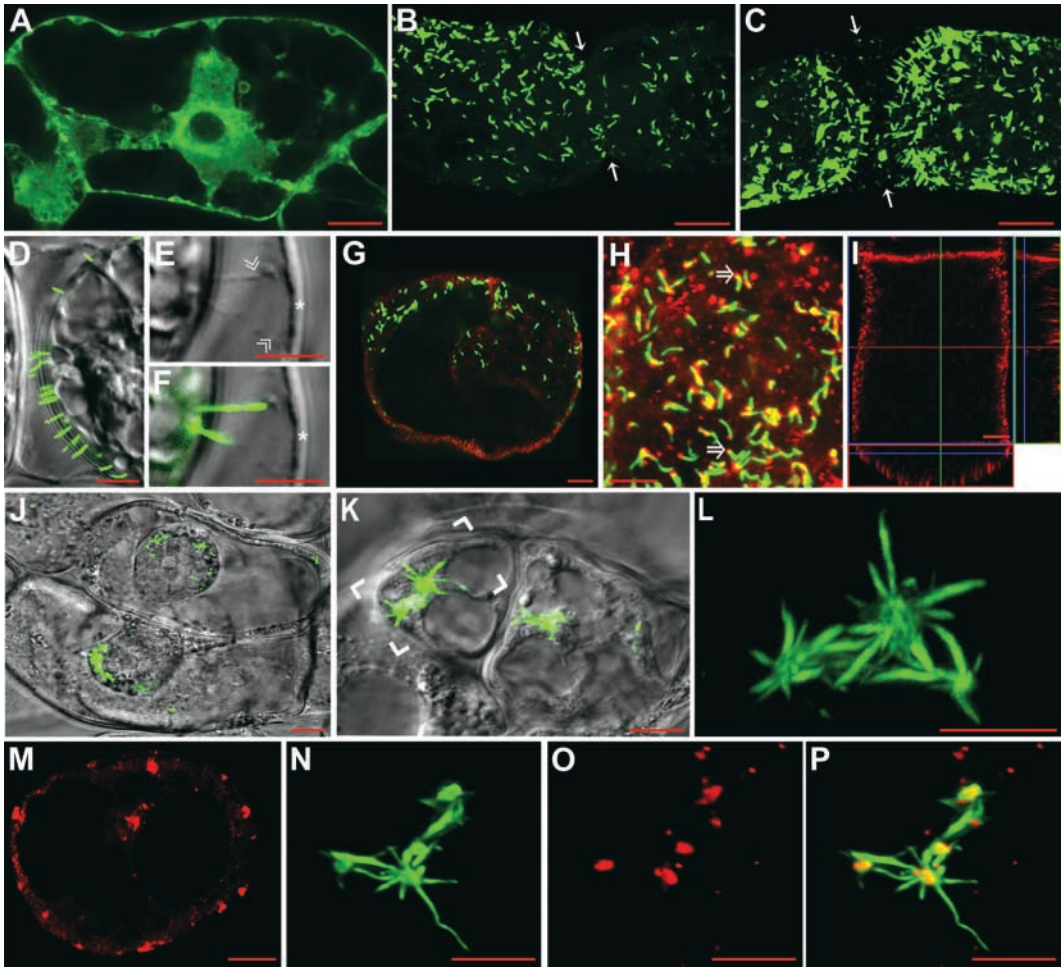

Figure 5. Involvement of the Endomembrane System and the Cytoskeleton in GFP:MP Targeting.

(A) Effect of BFA on GFP:MP distribution. BFA (10 μg/mL) was added 8 h after induction to block the secretory pathway, and cells were observed 16 h later. GFP:MP tubule formation is inhibited, and fluorescence is cytoplasmic.

(B) Effect of oryzalin on tubule formation. A total of 10 μM oryzalin was added 8 h after induction to depolymerize microtubules. Cells were observed 40 h later. Tubules formed over the entire cell surface instead of being localized specifically within the cross wall (arrows).

(C) to **(F)** Effect of plasmolysis on tubules in oryzalin-treated cells. Cells were observed at least 1 h after the addition of mannitol, when the lateral plasma membrane also had retracted from the side walls.

(C) Oryzalin-treated cells after plasmolysis. Protoplasts have retracted from the cell wall, giving rise to erect tubules that are not attached to the cross wall (cf. with **[B]**, in which the tubules are appressed to the cell wall). The position of the cross wall is indicated by arrows.

(D) Tubules have retracted from the walls together with the protoplast during plasmolysis. The tubules are erect and embedded within Hechtian strands connected to cross walls or side walls.

(E) Differential interference contrast (DIC) image showing Hechtian strands (double arrowheads) connected to a side wall (asterisk).

(F) Tubules are present within the Hechtian strands attached to side walls. Note that the tubules are not attached to the walls (asterisk).

(G) An oryzalin-treated induced cell fixed with glutaraldehyde and immunolabeled with tubulin antibodies (red). Microtubules are completely disassembled (red), whereas GFP:MP tubules (green) are visible at the cell surface.

(H) Distribution of GFP:MP tubules (green) and calreticulin-labeled structures (red) in an oryzalin-treated cell. Tubules formed over the entire cell surface, and most emerged from calreticulin-labeled spots (open arrows).

(I) Orthogonal view of the calreticulin-labeled structures in two neighboring wild-type BY-2 cells. Numerous calreticulin-labeled spots are present over the entire cell surface.

(J) to **(L)** Effects of the simultaneous disruption of microtubules and microfilaments on tubule formation.

(J) A total of 10 μM oryzalin and 2 μM latrunculin B were added 8 h after induction to depolymerize both microtubules and actin filaments. Cells were observed 40 h later. Under these conditions, tubules accumulated preferentially in the nucleus periphery.

(K) Cells containing aster-like tubules.

(L) Detailed view of the boxed region in **(K)**.

(M) Calreticulin-labeled structures in a cell treated with oryzalin and latrunculin.

(N) to **(P)** Aster-like tubules **(N)** and cytoplasmic calreticulin aggregates **(O)** in a cell treated with oryzalin and latrunculin. **(P)** shows the corresponding merged image.

Single optical sections are shown in **(A)**, **(D)** to **(G)**, **(J)**, and **(K)**. **(B)**, **(C)**, **(H)**, **(L)**, and **(N)** to **(P)** show projections of 27, 40, 7, 16, 19, and 45 sections, respectively. All optical sections were 0.45 μm thick except for those in **(N)** to **(P)** (0.1 μm). In **(D)** to **(F)**, **(J)**, and **(K)**, the GFP:MP channel and DIC images have been merged. Bars = 5 μm except in **(A)** to **(C)**, **(G)**, **(J)**, **(K)**, and **(M)** (10 μm).

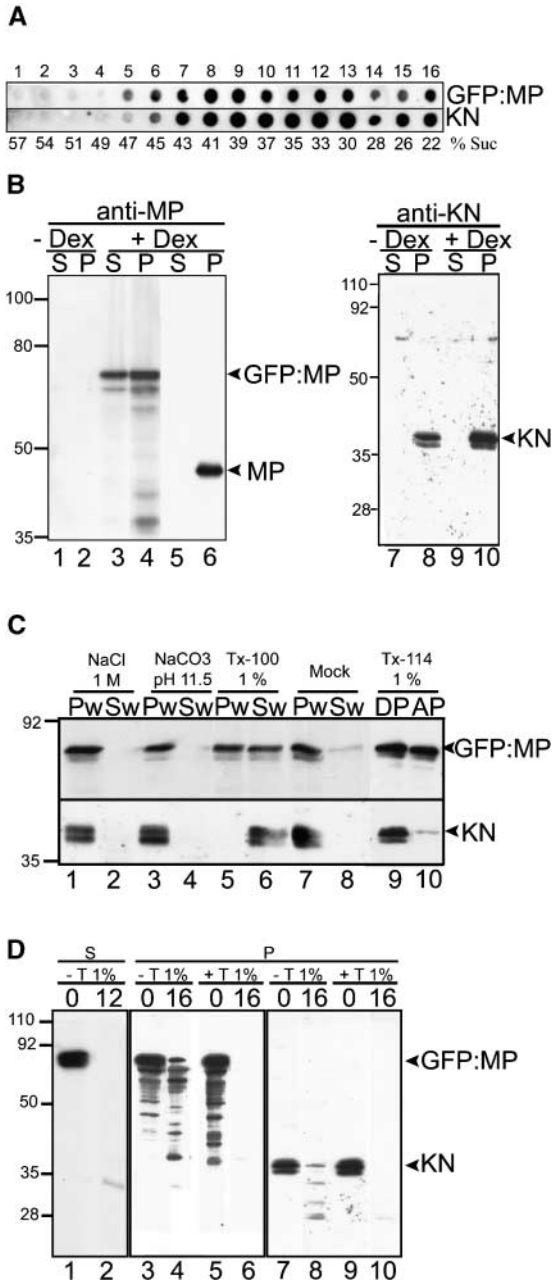

Figure 6. Biochemical Analysis of the GFP:MP Protein.

(A) Subcellular distribution of GFP:MP and KNOLLE (KN) in synchronized 2B15 cells as determined by dot blot analysis of fractions obtained after sedimentation in a 20 to 60% linear sucrose density gradient. Ten-microliter aliquots of each gradient fraction were probed with MP antibodies or with KNOLLE immunoglobulins. Fraction numbers are indicated at top, and the sucrose concentration in each fraction is indicated at bottom.

(B) Cell fractionation analysis of GFP:MP in extracts of noninduced and induced 2B15 cells and of MP in extracts from agroinfiltrated *N. benthamiana* leaves. Fractions correspond to the supernatant (S) and pellet (P) after centrifugation of cleared S10 extracts at 100,000*g*. Equal amounts (20 μg) of total protein from the S and P fractions were examined by immunoblot analysis using anti-MP (lanes 1 to 6) or anti-KNOLLE (lanes 7 to 10) antibodies. Lanes 1 and 2, noninduced 2B15 cells (−Dex); lanes 3 and 4, induced 2B15 cells 24 h after induction (+Dex); lanes 5 and 6, induced leaves 24 h after induction. Arrowheads indicate the positions of the 68-kD GFP:MP, the 38-kD MP, and KNOLLE proteins. Molecular mass markers (kD) are indicated at left.

(C) Membrane association of GFP:MP. Aliquots (250 μg) of the 100,000*g* P fraction were supplemented with 1 M NaCl (lanes 1 and 2), Na_2CO_3, pH 11.5 (lanes 3 and 4), 1% Triton X-100 (lanes 5 and 6), or buffer (lanes 7 and 8), incubated on ice for 60 min, and centrifuged again at 100,000*g* to give the Sw and Pw washed fractions. In lanes 9 and 10, 1 mg of protein from the P fraction was supplemented with 1% Triton X-114 in Tris buffer, incubated on ice, and centrifuged. The supernatant was incubated further at 37°C and centrifuged again to separate the detergent phase (DP) and the aqueous phase (AP). All fractions were examined by immunoblot analysis using anti-MP (top gel) or anti-KNOLLE (bottom gel) antibodies. Positions of the GFP:MP and KNOLLE proteins and molecular mass markers (kD) are indicated at right and left, respectively.

(D) Protease susceptibility of GFP:MP. Aliquots (100 μg) of the P and S fractions of induced 2B15 cells were incubated with proteinase K. As a control, soluble GFP:MP was incubated without (lane 1) or with (lane 2) added proteinase K (12 μg) in the absence of Triton X-100. In lanes 3 to 10, P fractions from induced cells were incubated without (lanes 3, 5, 7, and 9) or with (lanes 4, 6, 8, and 10) proteinase K (16 μg) and in the absence (−T 1%; lanes 3, 4, 7, and 8) or the presence (+T 1%; lanes 5, 6, 9, and 10) of 1% Triton X-100. Aliquots (20 μg) were examined by immunoblot analysis using anti-MP (lanes 1 to 6) or anti-KNOLLE (lanes 7 to 10) antibodies.

was very different from that observed in untreated or oryzalin-treated cells (Figure 5I), because small aggregates rather than punctate structures were detected at the cell surface and within the cytosol (Figure 5M). All aster-like tubule clusters showed calreticulin labeling in their centers, as if the tubules originated from these cytosolic foci (Figures 5N to 5P).

Together, these results indicate that a functional secretory pathway, but not the cytoskeleton, is required for tubule formation in BY-2 cells. Proper targeting of the MP to cross walls is strictly dependent on microtubules, whereas microfilaments seem to be essential for MP targeting to the cell surface when microtubules are disrupted. Our results also reveal that the sites of tubule assembly (whether MP tubules are formed at cross walls, as in control cells, at the cell periphery in the absence of microtubules, or within the cytosol upon the disruption of microtubules and microfilaments) always correlate with calreticulin-labeled foci, suggesting that tubule formation probably is not a random process but requires a specific environment.

Dual Behavior of the MP

To determine whether GFP:MP is associated with membranous structures, the subcellular distribution of GFP:MP was determined by sucrose density gradient centrifugation. GFP:MP was present in most sucrose gradient fractions of a crude cell extract from induced cells, although the highest levels were observed in fractions from the middle toward the lighter fractions of the gradient (Figure 6A). Interestingly, KNOLLE, which has been demonstrated to be an integral membrane protein (Lauber et al., 1997), was distributed similarly across the gradient (Fig-

ure 6A). In further experiments, extracts from noninduced and induced 2B15 cells as well as from agroinfiltrated *N. benthamiana* leaves were precentrifuged at 10,000*g* to eliminate heavy cell debris, and the supernatant was centrifuged further at 100,000*g* to give supernatant (S) and microsome pellet (P) fractions. Equal amounts of protein then were loaded onto SDS denaturing gels and examined by immunoblot analysis using MP-specific antibodies.

No signal was observed in noninduced cells (Figure 6B, lanes 1 and 2), whereas a 68-kD band corresponding to GFP:MP was detected in both S and P fractions from induced cells (Figure 6B, lanes 3 and 4) and a 38-kD band corresponding to MP was present exclusively in the P fraction from *N. benthamiana* leaves (Figure 6B, lanes 5 and 6). As judged by the relative intensities of the signals, GFP:MP was slightly more concentrated in the P fraction than in the S fraction. Because of the absence of MP in the S fraction from leaf extracts, we suggest that the soluble GFP:MP, which most likely contributes the weak diffuse cytoplasmic fluorescence observed in 2B15 cells (data not shown), is functionally irrelevant and probably the result of the presence of the hydrophilic domain of the GFP. Minor bands of lower molecular mass also were recognized by the MP-specific antiserum, especially in the P fraction from 2B15 cells, and presumably represent GFP:MP degradation products. By contrast, KNOLLE was found exclusively in the P fractions from both noninduced and induced 2B15 cells (Figure 6B, lanes 7 to 10), a distribution consistent with that of an integral membrane protein.

To further characterize the nature of the membrane association of the MP, P fractions were exposed to various solubilizing agents. Treatment at pH 11.5 or with 1 M NaCl released little or no GFP:MP (or MP; data not shown) from the P pellet (Figure 6C, lanes 1 to 4, top gel), as also observed for a buffer-treated control (Figure 6C, lanes 7 and 8, top gel). As expected, KNOLLE remained membrane bound under the same conditions (Figure 6C, lanes 1 to 4, 7, and 8, bottom gel). The addition of 1% Triton X-100 released only ~50% of the GFP:MP from the pellet, whereas KNOLLE was fully solubilized in the presence of this detergent (Figure 6C, lanes 5 and 6, top and bottom gels, respectively). Similarly, Triton X-114 phase partitioning resulted in an ~1:1 distribution of the GFP:MP between the detergent and aqueous phases (Figure 6C, lanes 9 and 10, top gel), whereas KNOLLE partitioned almost entirely in the detergent phase (Figure 6C, lanes 9 and 10, bottom gel). Identical behavior of MP also was observed when Triton X-114 phase partitioning was performed on the P fraction from *N. benthamiana* (data not shown). These experiments were repeated at least three times. Together, these results indicate that the MP probably exists in two forms, an integral membrane form and a more hydrophilic form that is nevertheless resistant to extraction at high salt or high pH.

To confirm that domains of the MP in the P fraction are embedded in membranes, we tested its susceptibility to proteolysis. S and P fractions prepared from induced 2B15 cells were subjected to proteinase K treatment for 5 min at 4°C before immunoblot analysis (Figure 6D). GFP:MP from the S fraction was degraded rapidly, as expected for a cytosolic protein (Figure 6D, lanes 1 and 2). Virtually no intermediate degradation products were observed. This is in marked contrast to the behavior of GFP:MP and KNOLLE from the P fraction, both of which were partially resistant to proteolysis degradation even at higher proteinase K concentrations (Figure 6D, lanes 3 and 4 for GFP:MP and lanes 7 and 8 for KNOLLE). For both proteins, proteolysis intermediates were abundant, presumably as a result of the partial protection of membrane-bound or intralumenal domains of GFP:MP (and KNOLLE). When the samples were treated first with Triton X-100, proteinase K completely degraded both GFP:MP and KNOLLE (Figure 6D, lanes 5 and 6 and lanes 9 and 10, respectively). Therefore, we conclude that, like KNOLLE (Lauber et al., 1997), GFP:MP in the P fraction is associated with membranes, with some domains of the protein exposed on the cytoplasmic side of vesicles, where they are accessible to proteolysis, whereas other domains are protected within the membrane bilayer or sequestered at the lumenal face.

GFP:MP and KNOLLE Coimmunoprecipitate

The colocalization of GFP:MP and KNOLLE observed in dividing cells (Figures 4H to 4J), together with the sucrose density gradient centrifugation and cell fractionation experiments described above, suggest that GFP:MP and KNOLLE might interact in vivo. Obviously, our results also support the idea that the MP could interact with calreticulin. To test these possibilities, we conducted coimmunoprecipitation studies. The P microsome fractions from noninduced and induced 2B15 cells were first treated with KNOLLE-, calreticulin-, or GFP-specific antibodies, and immunoprecipitated proteins were detected with GFP- (Figure 7A), KNOLLE- (Figure 7B), or calreticulin-specific antibodies (data not shown). Immunoprecipitation with either the KNOLLE- or GFP-specific antibodies resulted in the isolation of both GFP:MP (Figure 7A, lane 6, arrowhead) and KNOLLE (Figure 7B, lane 6, arrowhead). As expected, GFP antibodies also immunoprecipitated GFP:MP from induced 2B15 cells, as revealed by immunoblot analysis using MP antibodies (Figure 7C, lane 6). Under the same conditions, coimmunoprecipitation of calreticulin by GFP antibodies and vice versa was unsuccessful (data not shown).

The GFP:MP and KNOLLE proteins isolated by immunoprecipitation (Figures 7A to 7C, lanes 6) had the same electrophoretic mobility on protein gels as their counterparts from nonimmunoprecipitated P fractions (Figure 7A, lane 2; Figure 7B, lanes 1 and 2; Figure 7C, lane 2). Finally, it is noteworthy that neither GFP:MP nor KNOLLE was detected in control immunoprecipitations performed on P fraction from noninduced cells (Figures 7A to 7C, lanes 3 and 4) or when antibodies were omitted (protein A alone; Figures 7A to 7C, lanes 3 and 5). Therefore, we conclude that GFP:MP and KNOLLE are linked physically in vivo, either by direct interaction or by indirect interactions involving a bridging protein or copackaging in the same vesicles.

DISCUSSION

In this study, we used MP-transgenic BY-2 suspension cells to study the behavior of GFP-tagged GFLV MP and its targeting to cell wall–associated tubules in vivo. Previous work on GFLV

(Ritzenthaler et al., 1995b) and other viruses with tubule-forming MPs (Canto and Palukaitis, 1999; Huang and Zhang, 1999; Huang et al., 2000; Pouwels et al., 2002) was performed on either plant tissue or transfected protoplasts. The transgenic BY-2 cell line described here has a number of distinct advantages over the other two systems. (1) BY-2 cells can be transformed readily with Agrobacterium and are almost ideal in terms of growth rate and homogeneity (Geelen and Inze, 2001).

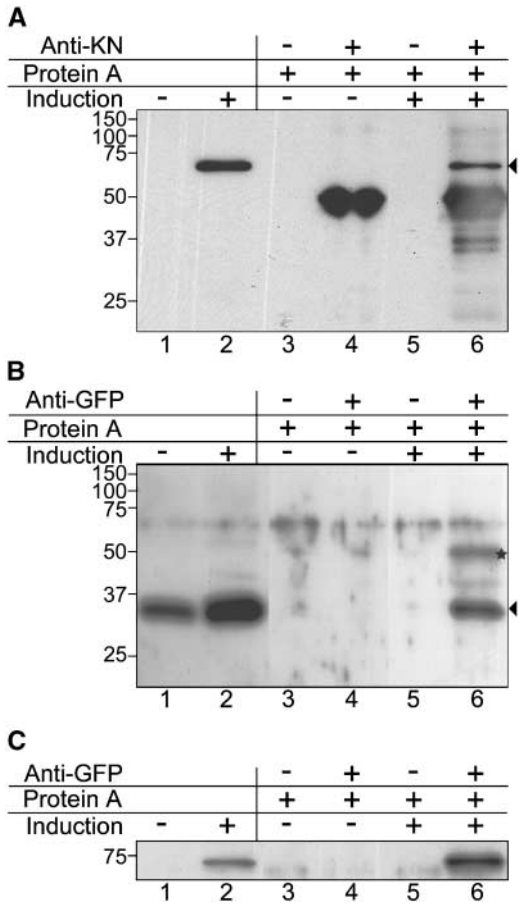

Figure 7. Coimmunoprecipitation of in Vivo–Expressed GFP:MP and KNOLLE.

The 100,000*g* P fractions from noninduced and induced 2B15 cells were examined by immunoblot analysis with antibodies directed against GFP **(A)**, KNOLLE (KN; **[B]**), or MP **(C)** either directly (lanes 1 and 2) or after immunoprecipitation with antibodies directed against KNOLLE (**[A]**, lanes 3 to 6) or GFP (**[B]** and **[C]**, lanes 3 to 6). The immunoprecipitation treatments performed on the different samples (with or without antibodies) are indicated in the tables above the gels. Arrowheads at right mark the positions of GFP:MP in **(A)** and KNOLLE in **(B)**. In **(A)** lane 4, the band corresponds to the ~50-kD anti-KNOLLE heavy chain immunoglobulins, which were recognized in lanes 4 and 6 by the goat anti-mouse immunoglobulins coupled to horseradish peroxidase used for immunodetection. The asterisk in **(B)** indicates an uncharacterized protein immunoprecipitated by the GFP antibodies and recognized by the KNOLLE antibodies. The positions of molecular mass markers (in kD) are indicated at left.

They also are excellent objects for CLSM investigations. (2) The behavior of GFP:MP in the transgenic BY-2 cells can be studied in isolation from other virus-encoded proteins, which evidently is not the case in virus-infected plant tissue. (3) Synchronous expression of GFP:MP in transgenic cells is achieved readily with an inducible promoter, which is impossible for whole-plant infections. (4) The cytoplasm of neighboring BY-2 cells is connected via plasmodesmata in their cross walls. This contrasts with the situation in protoplasts, which lack cell walls and plasmodesmata. (5) Finally, the presence of both cross and side walls in the BY-2 cells permits comparison of the behavior of the GFP:MP with respect to walls with and without plasmodesmata.

MP and Tubule Assembly

By immunoblot analysis, GFP:MP was clearly detectable 2 h after induction and steady state levels increased for at least 24 h. Detection of GFP:MP fluorescence occurred only later (~8 to 10 h after induction), with the appearance of cytoplasmic punctate structures and cross wall tubules that elongated progressively. This accumulation was slightly faster than that observed in GFLV-infected protoplasts, in which MP became detectable only after 18 h and tubules were seen only rarely before 30 h after infection (Ritzenthaler et al., 1995a, 1995b). We do not know exactly how the kinetics of the appearance of tubules in these experiments is related to the rate of cell-to-cell movement of GFLV in a natural infection. If there is a direct relation, however, it would indicate a rather slow movement of GFLV compared with TMV (reviewed by Heinlein, 2002).

Structurally, GFP:MP tubules are very similar to those observed in GFLV-infected plants (Ritzenthaler et al., 1995b). They have an internal diameter compatible with the passage of 28-nm virions, are lined with plasma membrane at their outer surface, and assemble at specific foci in an oriented manner. The only difference we detected between MP tubules produced from replicating GFLV in plant tissue and from GFP:MP in 2B15 cells was the absence of virions from the interior of the latter. Thus, the N-terminal GFP fusion to the MP has no effect on its targeting to the cell wall and on tubule formation per se. We also conclude that no other GFLV-coded protein is required for MP trafficking to the cell wall and tubule assembly, as observed for other members of the Comoviridae (Wellink et al., 1993), Caulimoviridae (Kasteel et al., 1996), Bunyaviridae (Storms et al., 1995), and Bromoviridae (Kasteel et al., 1997a). At present, we do not know if GFP:MP can support virus cell-to-cell movement in the context of a normal infection, although similar GFP:MP fusions for *Cucumber mosaic virus*, but not for *Alfalfa mosaic virus*, have been reported to be functional in cell-to-cell and long-distance movement (Canto and Palukaitis, 1999; Sánchez-Navarro and Bol, 2001).

Membrane Association of GFP:MP

Density gradient experiments revealed that GFP:MP fractionated similarly to KNOLLE, an integral membrane protein, and provide circumstantial evidence for the putative hydrophobic nature of the MP. (1) The presence of GFP:MP, MP, and

KNOLLE in the same microsomal fraction, (2) the failure of GFP:MP and KNOLLE to go into solution at high salt and high pH, and (3) the similar behavior of these two proteins toward proteolysis indicate that MP behaves like an integral membrane protein and strongly argue against the MP as a peripheral membrane protein candidate. Our results also exclude the possibility that MP membrane attachment could occur via a lipid anchor. This is corroborated by the absence of any of the necessary signal sequences known to date within the primary sequence of the MP (Thompson and Okuyama, 2000). On the contrary, all of our data suggest that MP is inserted into the lipid bilayer of membranes via a hydrophobic domain.

The MP of TMV has two putative α-helical transmembrane domains of ~20 amino acids (Brill et al., 2000). For CPMV, an LPL motif, also present in the MP of GFLV, was shown to be necessary for cell membrane targeting of the MP and for viral spread (Bertens et al., 2000). A computer-assisted search for signal peptides or typical membrane-spanning domains within the GFLV MP sequence was unsuccessful, although amino acids 33 to 50, 120 to 147, and 197 to 219 of the MP all showed a high degree of hydrophobicity (data not shown). Interactions between one or more of these hydrophobic regions and the lipid bilayer could anchor the MP to membranes, thereby shielding these regions from proteinase K degradation.

Confirmation that at least a fraction of the MP behaves as an intrinsic membrane protein has come from experiments performed with nonionic detergents. Consistent with its integral membrane nature (Lukowitz et al., 1996), KNOLLE was fully solubilized by Triton X-100 and partitioned almost completely in the Triton X-114 phase. Under the same conditions, only ~50% of GFP:MP was solubilized by Triton X-100 or partitioned in the Triton X-114 phase. Equivalent dual partitioning also was observed with MP alone. Thus, MP appears to exist in two forms, one that behaves as an integral membrane protein and a more hydrophilic form that becomes solubilized by nonionic detergent but not by high salt or at high pH. Similar anomalous behavior during partitioning has been described for other proteins (Sanchez-Ferrer et al., 1994). Insertion into lipid rafts is one of the many possibilities that could explain the anomalous partitioning behavior of the MP (Simons and Ikonen, 1997; Brown and London, 1998). However, in plants, there is no strong evidence for the existence of lipid rafts. Furthermore, insertion of proteins into these specific domains of the plasma membrane of other organisms is largely the result of posttranslational acylation at Cys residues (Brown and London, 1998), the only amino acid absent from the MP.

The anomalous partitioning behavior of the MP also could be a consequence of the ability of the protein to self-assemble into tubules, as shown for the MP of CPMV (Kasteel et al., 1997b). Thus, it is possible that, upon treatment with Triton X-114, a fraction of the solubilized MP oligomerizes by interaction of the hydrophobic domains. The masked hydrophobic domains then would no longer be available to drive the insertion of the MP into micelles, leading to its partitioning in the aqueous phase. Similar behavior has been observed for a number of integral membrane proteins, such as synaptotagmin I and vinculin (Ziegler et al., 2002; Wu et al., 2003). Alternatively, changes in the phosphorylation status of the MP might lead to changes in its hydrophobicity, as in the case of pp60c-src membrane-associated Tyr kinase, which is translocated from the plasma membrane to the cytosol by phosphorylation (Walker et al., 1993). Consistent with this idea, gating of the TMV MP was shown to depend in vivo on phosphorylation in a host-dependent manner (Waigmann et al., 2000). At present, we have no evidence that the GFLV MP is phosphorylated in vivo. However, multiple electrophoretic variants of the MP often are observed (Ritzenthaler et al., 1995a; this work) and could reflect changes in the phosphorylation state of the protein. Finally, pH-induced conformational changes also have been shown to confer the capacity to integrate into membranes. Examples are seen in clathrin (Maezawa et al., 1989), *Human rhinovirus type 2* (Brabec et al., 2003), and *Influenza virus* hemagglutinin (Remeta et al., 2002).

Polarized Targeting of MP to Cross Walls and the Cell Plate

Our experiments with transgenic BY-2 cells have demonstrated that GFP:MP localizes predominantly either to highly modified plasmodesmata in the cross walls of interphase cells or to the cell plate in dividing cells. Additional weaker punctate labeling also was observed in the cytoplasm of interphase cells. Except for the targeting to plasmodesmata, this intracellular distribution is similar to that observed for KORRIGAN, a membrane-bound endo-1,4-β-glucanase essential for cytokinesis in Arabidopsis (Zuo et al., 2000). As demonstrated by the requirement for specific sorting signals residing within the cytosolic tails for the proper targeting of KORRIGAN, there is strong evidence that trafficking of KORRIGAN occurs by a polarized mechanism rather than by mistargeting (Zuo et al., 2000). In view of the similarity of the subcellular localization of GFP:MP and KORRIGAN, we suggest that GFP:MP also might be targeted in a polarized manner.

Polarized targeting of KORRIGAN depends largely on dileucine (LL) and YXXΦ motifs (where Y refers to Tyr, X refers to any amino acid residue, and Φ refers to hydrophobic residues with a bulky side chain). Interestingly, not only are these motifs responsible for the binding of clathrin-coated vesicle adaptor complexes at the plasma membrane and Golgi apparatus in both animal and plant cells (Holstein, 2002; Bonifacino and Lippincott-Schwartz, 2003), they also appear to confer specific localization to numerous members of the syntaxin family of proteins in mammalian cells, also referred to as SNAREs (soluble *N*-ethylmaleimide–sensitive factor attachment protein receptors) (Mellman, 1996; Marks et al., 1997; Tang and Hong, 1999). KNOLLE is a well-known member of the plant syntaxin family and also contains potential LL and YXXΦ sorting motifs (Zuo et al., 2000). Here, we have shown that KNOLLE-specific antibodies immunoprecipitate GFP:MP and vice versa, indicating that these two proteins interact either directly or indirectly (i.e., copackaging into the same vesicles). This observation could indicate that during cytokinesis, KNOLLE may contribute to the targeting of GFP:MP to the cell plate.

During interphase, however, the expression of KNOLLE is repressed severely (Lukowitz et al., 1996; Lauber et al., 1997), so the likelihood that KNOLLE contributes to the transport of the MP in nondividing cells is very low. In fact, we present evidence

that GFP:MP targeting to cross walls can occur independently of cytokinesis, as shown by the presence of tubules in both young and older cross walls in 2B15 cell chains (Figure 4A) or in the walls of caffeine-treated cells that had not undergone cell division (Figure 4B). Moreover, the presence of tubular structures within the walls of agroinfiltrated *N. benthamiana* epidermal cells from mature leaves is convincing evidence that a KNOLLE-independent mechanism of GFP:MP targeting to the cross walls must exist.

We noted recently that putative LL and YXXΦ motifs are present near the N terminus of the GFLV MP sequence. Sequence comparisons have revealed a high degree of conservation of these motifs among different GFLV isolates and in the MPs of other nepoviruses, including *Arabis mosaic virus*, *Olive latent ringspot virus*, *Grapevine chrome mosaic virus*, *Tomato black ring virus*, *Cycas necrotic stunt virus*, and *Strawberry mottle virus* (our unpublished data). It is possible that these motifs may represent intrinsic MP transport signals that govern MP intracellular movement.

Mode(s) of MP Transport

To address the question of how MP targeting and tubule formation could occur in cells, intracellular trafficking of the MP was studied in dividing and nondividing cells. It is clear from the experiment using agroinfiltration of mature leaf cells that the capacity of the MP to be targeted to walls (presumably plasmodesmata) and to assemble into tubules is cell cycle independent. Whether the cellular mechanisms involved in MP targeting and tubule formation would be similar in cells that have the capacity to divide is a question we addressed in BY-2 cells. Inducible expression of GFP:MP in BY-2 cells also offered the possibility, not available with leaf cells, to study the targeting of the MP to cross walls versus side walls.

In interphase BY-2 cells, GFP:MP fluorescence was localized mainly in cross wall tubules, although discrete cytoplasmic punctate structures also were visible. During cytokinesis, GFP:MP accumulates almost exclusively within the cell plate. Targeting to the plane of division also was observed in BY-2 cells when MP was expressed from replicating virus, thereby eliminating GFP as being responsible for the GFP:MP accumulation within the cell plate. Furthermore, this finding suggests strongly that cell plate targeting is relevant to the movement of the virus in planta. In particular, it could account for the ability of some nepoviruses to invade meristematic tissues (Walkey and Webb, 1968).

It is well known that Golgi-derived secretory vesicles associate with phragmoplast microtubules during their delivery to the equatorial plane of the dividing cell. Presumably, with the help of KNOLLE, these vesicles fuse with one another to form a membrane network that matures centrifugally into a disc-shaped cell plate that eventually fuses with the parental cell wall (reviewed by Staehelin and Hepler, 1996; Verma, 2001). This maturation process can be blocked specifically by caffeine, which prevents secretory vesicle fusion without affecting their transport to the cell plate (Samuels and Staehelin, 1996; Valster and Hepler, 1997). A similar phenotype is obtained in KNOLLE embryo-lethal knockout Arabidopsis (Lukowitz et al., 1996). As in the KNOLLE protein, targeting of GFP:MP to normal and aborted cell plates occurred in both untreated and caffeine-treated BY-2 cells, respectively. Therefore, and keeping in mind that KNOLLE traffics along microtubules from Golgi stacks to the cell plate at the surface of secretory vesicles (Völker et al., 2001), we hypothesize that in BY-2 cells MP follows essentially the same pathway to its final destination, most likely plasmodesmata. According to this model, we predict that inhibition of secretion and disruption of the microtubular cytoskeleton both should affect MP intracellular trafficking. Indeed, this prediction is supported by our observations.

BFA is a fungal metabolite whose inhibitory action on secretion leads to the resorption of the Golgi apparatus into the ER (Nebenführ et al., 2002; Ritzenthaler et al., 2002b). In agreement with our model, application of BFA led to the inhibition of tubule formation and to the redistribution of GFP:MP within the cytosol. Similarly, targeting of the TMV MP to punctate structures associated with the cortical ER was prevented in the presence of BFA, and MP was redistributed within the cell (Heinlein et al., 1998). Inhibition of tubule formation also was observed upon BFA treatment of protoplasts expressing the MPs of CPMV or *Cauliflower mosaic virus* (Huang et al., 2000; Pouwels et al., 2002). For CPMV, however, BFA led to the accumulation of the MP in an ER-like compartment (Pouwels et al., 2002). Thus, although a functional endomembrane system appears to be essential for the proper targeting of MP, BFA treatment seems to exert different effects on the localization of these viral proteins. This finding could reflect variations in the way MPs attach to endomembranes and where this occurs, either early or late along the secretory pathway. Consistent with this notion, TMV MP and possibly CPMV MP seem to bind to ER membranes (Heinlein et al., 1998; Pouwels et al., 2002), whereas GFLV MP seems to be targeted to other membranes further downstream along the secretory pathway. Therefore, it is possible that the punctate fluorescent structures observed in the cytosol in our studies correspond to secretory vesicles en route to the cross wall.

Our results also clearly reveal the requirement for a functional cytoskeleton for the proper delivery of MP but not for tubule assembly. Thus, although disruption of the cytoskeleton did not prevent tubule formation, it had profound effects on the sites of tubule assembly. In particular, microtubules seem to be essential for the correct delivery of the MP to cross walls, as revealed by the improper targeting of the MP when microtubules were depolymerized but not when they were stabilized. Normal targeting to cross walls in taxol-treated cells can be explained by the fact that stabilized microtubules remain competent for the transport of membranes via motor proteins (Roux et al., 2002).

It is less evident why GFP:MP is delivered exclusively to Hechtian attachment sites at cross walls in untreated cells but also to side wall Hechtian attachment sites under conditions in which microtubules are depolymerized. In contrast to the microtubule-dependent trafficking of vesicles to the cell plate during cytokinesis, it is known that vesicle trafficking to the cell surface continues in the absence of microtubules (Steinborn et al., 2002). On the other hand, studies with actin-disrupting drugs have suggested a role for microfilaments in vesicle trafficking to the plasma membrane but not to the cell plate

(Geldner et al., 2001). Thus, it is possible that MP traffics along two different pathways depending on the status of the cytoskeleton: a microtubule-dependent pathway in normal cells and a microfilament-dependent default pathway when microtubules are depleted. Clear support for this hypothesis is provided by (1) the normal targeting of GFP:MP in cells with depolymerized microfilaments and (2) the formation of tubules in the cytosol (often the nuclear periphery) under conditions in which both microtubules and microfilaments are disrupted. There is no reason to believe that this transport model applies only to dividing cells, because no differences were detected between BY-2 cells and leaf cells in their capacity to form tubules and to traffic the MP, apart from the preferential targeting of the MP to the youngest cross walls in BY-2 cells. This latter phenomenon could simply be a consequence of the preferential (but not exclusive) flow of vesicles to the youngest cross walls, which are still undergoing maturation, rather than to older ones that have already completed this maturation process.

A Receptor for MP Targeting and/or Tubule Assembly?

An important issue that remains to be addressed is why tubules assemble at specific sites within cells. We have shown that at least four sites in BY-2 cells provide a favorable environment for tubule formation: specific foci within cross walls (1) and side walls (2) in normal and microtubule-disrupted cells, respectively; (3) the aborted cell plate upon caffeine treatment; and (4) specific sites within the cytosol in cells with microtubule- and microfilament-disrupted cytoskeletons. Thus, it is very unlikely that tubule formation results from a random process; rather, it is the consequence of an interaction with intracellular receptor(s). Considering the numerous features for intracellular transport of the MP that we have established in our investigation, we can envisage two types of receptors: a receptor responsible for correct targeting/docking of the MP-carrying secretory vesicles, and/or a receptor required for the nucleation/assembly of tubules.

A protein that has some of the predicted properties of a candidate MP receptor is calreticulin, whose localization varied from specific foci at the cell surface (presumably Hechtian attachment sites) in normal or microtubular defective cells to small cytosolic and pericellular aggregates upon disruption of both microtubules and microfilaments. Even under conditions in which the GFP:MP tubules assembled into aster-like structures within the cytosol, calreticulin labeling always was found at their base. Calreticulin has been shown to be an essential modulator for integrin-mediated adhesion to RGD-containing extracellular matrix substrates such as fibronectins and laminins in mammals (Coppolino et al., 1997). In plants, plasma membrane adhesion to the cell wall also is mediated by integrin-like proteins containing RGD binding sites (Canut et al., 1998). The nature of the proteins that participate in membrane–wall adhesion in plants, their spatial localization relative to Hechtian attachment sites, and the potential role of calreticulin in membrane–wall adhesion remain to be discovered. It may be significant, however, that *Turnip crinkle virus* MP has been shown by two-hybrid analysis to interact with RGD-containing polypeptides (Lin and Heaton, 2001) and that TMV MP is targeted to putative cell wall adhesion sites in protoplasts (Heinlein et al., 1998). However, we cannot conclude at present that calreticulin is a receptor for GFLV MP targeting or tubule nucleation, because it may simply be a component of a complex that always happens to be associated with tubules. Consistent with this finding, we were unable to coimmunoprecipitate calreticulin and MP. We are currently using gene silencing to test for an involvement of plant calreticulin in cell adhesion and in GFLV MP targeting and tubule formation.

METHODS

pTA7002-GFP:MP Cloning

Cloning procedures were as described by Sambrook et al. (1989). The GFP gene of plasmid pCK-GFP:2B (Gaire et al., 1999) was replaced by the EGFP gene from plasmid pEGFP (Clontech, Heidelberg, Germany) using the NcoI and KpnI sites to give plasmid pCK-EGFP:2B. The open reading frames encoding EGFP:2B and 2B in pCK-EGFP:2B were amplified by PCR using the primers P4624b (5′-AAA**GCTAGC**TTATCTCACGGTTGAG-3′) and P4627b (5′-AAAGATCTCGAGAACAATGGTGAGCAAGGGCGAGG-3′), and P4624b and P4639b (5′-AAAGATCTCGAGAACAATGGCGGATGGGAAGACTAC-3′), respectively. The PCR products were digested with XhoI (underlined) and NheI (boldface) and ligated into the XhoI-SpeI sites of plasmid pTA7002 (Aoyama and Chua, 1997) to give pTA7002-GFP:MP and pTA7002-MP. All clones obtained were verified by sequence analysis.

Tobacco BY-2 Cell Transformation, Culture, and Synchronization

Clonal BY-2 tobacco (*Nicotiana tabacum* cv BY-2 [Bright Yellow 2]) cell cultures (Nagata et al., 1992) transgenic for the pTA7002-GFP:MP construct were established by *Agrobacterium tumefaciens*–mediated transformation (Criqui et al., 2000). Expression of GFP:MP in the transgenic cell lines was induced by the addition of 10 μM dexamethasone (Sigma) to the BY-2 culture medium. Selection of cell line 2B15 was based on epifluorescence screening of individual transformed calli.

Cells were synchronized as described (Yasuhara et al., 1993) with modifications. Seven-day-old 2B15 cells (20 mL) were mixed with 3 volumes of fresh BY-2 medium in the presence of aphidicolin (Sigma) at 3 μg/mL. After 24 h at 27°C, cells were washed with 1 L of 4% sucrose in water for 30 min and resuspended in BY-2 medium for 6 to 7 h. When mitotic cells began to appear, propyzamide (3.5 μM) and dexamethasone were added to the medium, and the cells were maintained at 18°C for 16 h. The cells then were washed with 1 L of 4% sucrose solution, resuspended in fresh BY-2 medium containing dexamethasone, and maintained at 18°C until a majority of the cells reached the telophase stage. The progression of the cells into mitosis was monitored by 4′,6-diamidino-2-phenylindole dilactate (1 μg/mL) staining in 0.1% Triton X-100.

Plasmolysis and Chemical Treatments

Plasmolysis was performed in BY-2 medium supplemented with 0.45 M mannitol. Metabolic inhibitors were added 8 h after induction at the following concentrations: oryzalin, 10 μM; cytochalasin, 20 μM; latrunculin B, 2 μM; taxol, 2 μM; and brefeldin A, 10 μg/mL. Observations were performed 24 h after the addition of the inhibitors. For caffeine treatment, cells were preincubated for 24 h in BY-2 medium containing 10 mM caffeine followed by 24 h of dexamethasone induction in the presence of caffeine.

Total Protein Extraction and Sucrose Gradient Fractionation

Total proteins from noninduced and induced synchronized 2B15 cells were extracted with 5 volumes of acetone. After 30 min of centrifugation at 10,000*g*, pellets were washed twice with acetone, dried, resuspended in SDS-PAGE loading buffer, and subjected to immunoblot analysis.

For sucrose gradient fractionation, 50 mL of synchronized cells was harvested 24 h after induction and centrifuged at 80*g* for 5 min, and the pellet was homogenized in 20 mL of homogenization buffer (40 mM Hepes KOH, pH 7.4, 10 mM KCl, 320 mM sucrose, 1 mM DTT, and 3 mM $MgCl_2$) supplemented with Complete Protease Inhibitor Cocktail (Roche Diagnostics, Meylan, France). The homogenate was passed through a nitrogen disruption bomb at 120 bar (Parr Instrument, Mokine, IL) and clarified by centrifugation at 10,000*g* for 10 min at 4°C. A total of 500 μL of the 10,000*g* supernatant (S10) was loaded on a 12.5-mL sucrose gradient (20:60%, w/v) in homogenization buffer and centrifuged for 18 h at 100,000*g*. Sixteen fractions of 0.8 mL each were collected, and the sucrose concentration was determined by refractometry. Ten-microliter aliquots of each fraction were dotted onto an Immobilon P membrane, and immunodetection of GFP:MP and KNOLLE on the membranes was as described below.

Treatment with Salts, Detergent, and Proteinase K

To test for the membrane association of GFP:MP protein, homogenates of synchronized noninduced and induced 2B15 cells were subjected to subcellular fractionation. For this, the S10 supernatant (see above) was centrifuged at 100,000*g* for 60 min to give a soluble fraction (S) and a microsomal pellet (P). The pellet was resuspended in the homogenization buffer. Protein concentrations of the S and P fractions were determined by the Bradford (1976) method. Equal amounts of protein (300 μg) were treated with homogenization buffer without additives (control) or supplemented with 1% Triton X-100, 1 M NaCl, or 0.1 M Na_2CO_3, pH 11.5. The samples were incubated on ice for 60 min and centrifuged again at 100,000*g* for 60 min, giving a Sw wash supernatant and a Pw wash pellet. The Sw wash supernatant was precipitated with 5 volumes of chloroform:methanol (1:4), and the resulting pellet and the Pw wash pellet were resuspended in 300 μL of protein loading buffer. Aliquots (20 μL) were fractionated by electrophoresis on a 12.5% SDS-PAGE gel and electrotransferred onto an Immobilon P membrane. Immunodetection was performed as described below.

For proteinase K digestion, the S and microsomal (P) fractions (100 μg of protein) were incubated with 12 and 16 μg of proteinase K (Sigma), respectively. Incubation was performed in 50 μL of homogenization buffer for 5 min on ice in the presence or absence of 1% Triton X-100. The reaction was stopped by adding 50 μL of protein loading buffer and boiling for 5 min. Twenty-microliter aliquots were loaded on a 12.5% SDS-PAGE gel and electrotransferred onto an Immobilon P membrane. Immunodetection was as described below.

Triton X-114 Phase Partitioning

One milligram of protein from the 100,000*g* pellet was resuspended in 0.5 mL of 50 mM Tris-HCl, pH 7.4, 1 mM DTT, and 1% Triton X-114. The suspension was kept on ice for 30 min with periodic vortexing and centrifuged for 20 min at 16,000*g*. The supernatant was incubated at 37°C for 15 min and subsequently centrifuged at room temperature for 5 min at 16,000*g* to separate the detergent and aqueous phases.

Plant Infiltration

Agrobacterium containing the pTA7002-GFP:MP construct was grown to saturation in Luria-Bertani medium. The culture was centrifuged and resuspended in 10 mM $MgCl_2$, 10 mM Mes, and 150 μM acetosyringone and kept at room temperature for 2 h. The culture then was diluted to 1 OD unit and infiltrated to the abaxial side of a leaf using a 2-mL syringe without a needle. Three days after infiltration, plants were sprayed with an aqueous solution containing 30 μM dexamethasone and 0.01% Tween 20. Samples were collected 24 h after induction and processed further for confocal laser scanning microscopy or subcellular fractionation.

Protoplast Transfection

Protoplast transfection was performed as described by Ritzenthaler et al. (2002a).

Coimmunoprecipitation Assay

Proteins from P fractions of synchronized noninduced and induced 2B15 cells were used for coimmunoprecipitation assays essentially as described (Blanar and Rutter, 1992). Briefly, GFP:MP or KNOLLE present in the P fractions (70 μg of total protein) was immunoprecipitated using mouse monoclonal anti-GFP immunoglobulins (Roche Diagnostics) diluted 1:2500 or rabbit anti-KNOLLE antibodies (Rose Biotech, Winchendon, MA) at 1:2500 dilution, respectively. Before the addition of the P fraction, protein A–Sepharose (Amersham Pharmacia) and antibodies were preincubated for 1 h at room temperature in coimmunoprecipitation buffer consisting of PBS, pH 7.5, supplemented with 5 mM EDTA, pH 8, 10% glycerol, 0.1% Tween 20, and 1 mM DTT. After three washes in the same buffer, the protein A–Sepharose–bound antibodies were mixed with P fractions (70 μg of protein), incubated overnight at 4°C with gentle agitation, and finally washed three times with coimmunoprecipitation buffer. The washed pellets were resuspended in 50 μL of protein blot buffer (Bio-Rad), and 20 μL was subjected to electrophoresis on SDS polyacrylamide gels followed by electrotransfer to an Immobilon P membrane. Immunodetection was as described below.

Immunoblot Analysis

After transfer, membranes were probed with affinity-purified GFLV MP–specific antibodies (Ritzenthaler et al., 1995a) diluted 1:10,000, anti-KNOLLE antibodies diluted 1:80,000, and anti-GFP monoclonal antibodies (Roche Diagnostics) diluted 1:8000. The immunoreactive proteins were detected using alkaline phosphatase– or horseradish peroxidase–conjugated goat anti-rabbit or goat anti-mouse antibodies at 1:5000 dilution and the enhanced chemiluminescence immunoblotting analysis system from Bio-Rad or Roche, respectively.

Immunofluorescence Labeling

BY-2 cells 4 days after subculture and overnight induction were fixed and processed for immunofluorescence labeling (Ritzenthaler et al., 2002b). Primary antibody dilutions were as follows: calreticulin, 1:1000 (Napier et al., 1995); anti-KNOLLE, 1:1000; and anti-β-tubulin, 1:300 (Amersham Pharmacia Biotech, Orsay, France). Secondary antibodies (Alexa Fluor 568 goat anti-rabbit or anti-mouse IgG; Molecular Probes, Leiden, The Netherlands) were used at 1:300 dilution.

Confocal Laser Scanning Microscopy

Before observation, fixed cells were mounted in a chamber containing PBS and 0.1% Na ascorbate, pH 7.4, to reduce photobleaching. The living cells were allowed to settle onto a poly-L-Lys–coated cover slip, which then was mounted in a perfusion chamber with a continuous supply (0.5 mL/min) of fresh BY-2 medium with or without supplementary

0.45 M mannitol. Cells were observed with a Zeiss LSM510 laser scanning confocal microscope (Jena, Germany) using a C-APOCHROMAT (×63 1.2 numerical aperture water immersion lens) in multitrack mode. Excitation/emission wavelengths were 488/505 to 545 nm for GFP and 543/long-pass 560 nm for Alexa Fluor 568. Transmitted light reference images were captured using differential interference contrast optics and argon laser illumination at 488 nm. The images are presented as single sections or stacks of neighboring sections as stated in the figure legends. LSM 510 three-dimensional reconstruction functions were used to compute projections of serial confocal sections. Image processing occurred in LSM510 version 2.8 (Zeiss) and Photoshop 6.0 (final image assembly; Adobe Systems, San Jose, CA).

Electron Microscopy

Cells were fixed with 2% glutaraldehyde in culture medium for 15 min at room temperature, centrifuged at 80*g* for 5 min, and transferred to 1 mL of fixative solution containing 2% glutaraldehyde and 0.1 mL of saturated picric acid in 25 mM potassium phosphate buffer, pH 7.4. Incubation was at 4°C for 16 h. After four washes in 25 mM potassium phosphate, pH 7.4, at room temperature, the cells were transferred to a secondary fixative containing 2% (w/v) osmium tetroxide and 0.5% (w/v) potassium ferrocyanide in 25 mM phosphate, pH 7.4, for 2 h at room temperature. The cells then were washed twice in phosphate buffer and twice in distilled water before transfer to 2% (w/v) aqueous uranyl acetate for 16 h at 4°C. After washing, the cells were dehydrated in an acetone series and embedded in Spurr's resin for ultrastructural analysis or in London Resin White (Plano, Marburg, Germany) for immunocytochemistry.

Immunocytochemistry

Ultrathin sections (40 to 60 nm) from heat-polymerized London Resin White blocks were cut on a Leica Ultracut UCT microtome (Bensheim, Germany). Immunogold labeling was performed as described previously (Bauly et al., 2000) using GFP antibodies (Molecular Probes) at a primary dilution of 1:20. Colloidal gold–coupled (10 nm) secondary antibodies were used at a dilution of 1:30. Uranyl acetate–poststained sections were examined with a Philips CM10 electron microscope (Eindhoven, The Netherlands) operating at 80 kV.

Upon request, materials integral to the findings presented in this publication will be made available in a timely manner to all investigators on similar terms for noncommercial research purposes. To obtain materials, please contact C. Ritzenthaler, christophe.ritzenthaler@ibmp-ulp.u-strasbg.fr.

ACKNOWLEDGMENTS

We are indebted to Ken Richards for critical reading of the manuscript, and we are grateful to Andy Maule for helpful discussions. We also thank R.M. Napier (Warwick, UK) for providing calreticulin antibodies and N.-H. Chua (New York, NY) for providing the pTA7002 plasmid. Moët and Chandon (Epernay, France) are thanked for their continued interest and financial support. This work was supported by the Centre National de la Recherche Scientifique (CNRS), the Ministère de la Jeunesse de l'Education Nationale et de la Recherche (to C.L.), the German-French Academic Exchange Program PROCOPE (04614PE), the German Research Council, and Université Louis Pasteur (Strasbourg). The Inter-Institute Zeiss LSM510 confocal microscopy platform was cofinanced by the CNRS, Université Louis Pasteur, the Région Alsace, the Association de la Recherche sur le Cancer, and the Ligue Nationale contre le Cancer.

Received May 21, 2003; accepted July 15, 2003.

REFERENCES

Akashi, T., Izumi, K., Nagano, E., Enomoto, M., Mizuno, K., and Shibaoka, H. (1988). Effects of propyzamide on tobacco cell microtubules *in vivo* and *in vitro*. Plant Cell Physiol. **29,** 1053–1062.

Aoyama, T., and Chua, N. (1997). A glucocorticoid-mediated transcriptional induction system in transgenic plants. Plant J. **11,** 605–612.

Baluška, F., Samaj, J., Napier, R., and Volkmann, D. (1999). Maize calreticulin localizes preferentially to plasmodesmata in root apex. Plant J. **19,** 481–488.

Bauly, J., Sealy, I., Macdonald, H., Brearley, J., Droge, S., Hillmer, S., Robinson, D., Venis, M., Blatt, M., Lazarus, C., and Napier, R. (2000). Overexpression of auxin-binding protein enhances the sensitivity of guard cells to auxin. Plant Physiol. **124,** 1229–1238.

Bertens, P., Wellink, J., Goldbach, R., and van Kammen, A. (2000). Mutational analysis of the cowpea mosaic virus movement protein. Virology **267,** 199–208.

Blanar, M., and Rutter, W. (1992). Interaction cloning: Identification of a helix-loop-helix zipper protein that interacts with c-Fos. Science **256,** 1014–1018.

Bonifacino, J., and Lippincott-Schwartz, J. (2003). Coat proteins: Shaping membrane transport. Nat. Rev. Mol. Cell Biol. **4,** 409–414.

Boyko, V., Ashby, J., Suslova, E., Ferralli, J., Sterthaus, O., Deom, C., and Heinlein, M. (2002). Intramolecular complementing mutations in tobacco mosaic virus movement protein confirm a role for microtubule association in viral RNA transport. J. Virol. **76,** 3974–3980.

Boyko, V., Ferralli, J., Ashby, J., Schellenbaum, P., and Heinlein, M. (2000a). Function of microtubules in intercellular transport of plant virus RNA. Nat. Cell Biol. **2,** 826–832.

Boyko, V., Ferralli, J., and Heinlein, M. (2000b). Cell-to-cell movement of TMV RNA is temperature-dependent and corresponds to the association of movement protein with microtubules. Plant J. **22,** 315–325.

Brabec, M., Baravalle, G., Blaas, D., and Fuchs, R. (2003). Conformational changes, plasma membrane penetration, and infection by human rhinovirus type 2: Role of receptors and low pH. J. Virol. **77,** 5370–5377.

Bradford, M.M. (1976). A rapid and sensitive method for the quantitation of microgram quantities of protein utilizing the principle of protein-dye binding. Anal. Biochem. **72,** 248–254.

Brill, L., Nunn, R., Kahn, T., Yeager, M., and Beachy, R. (2000). Recombinant tobacco mosaic virus movement protein is an RNA-binding, alpha-helical membrane protein. Proc. Natl. Acad. Sci. USA **97,** 7112–7117.

Brown, D., and London, E. (1998). Functions of lipid rafts in biological membranes. Annu. Rev. Cell Dev. Biol. **14,** 111–136.

Canto, T., and Palukaitis, P. (1999). Are tubules generated by the 3a protein necessary for *Cucumber mosaic virus* movement? Mol. Plant-Microbe Interact. **12,** 985–993.

Canut, H., Carrasco, A., Galaud, J., Cassan, C., Bouyssou, H., Vita, N., Ferrara, P., and Pont-Lezica, R. (1998). High affinity RGD-binding sites at the plasma membrane of *Arabidopsis thaliana* links the cell wall. Plant J. **16,** 63–71.

Coppolino, M., Woodside, M., Demaurex, N., Grinstein, S., St-Arnaud, R., and Dedhar, S. (1997). Calreticulin is essential for integrin-mediated calcium signalling and cell adhesion. Nature **386,** 843–847.

Coue, M., Brenner, S., Spector, I., and Korn, E. (1987). Inhibition of actin polymerization by latrunculin A. FEBS Lett. **213,** 316–318.

Criqui, M., Parmentier, Y., Derevier, A., Shen, W., Dong, A., and Genschik, P. (2000). Cell cycle-dependent proteolysis and ectopic overexpression of cyclin B1 in tobacco BY2 cells. Plant J. **24,** 763–773.

Ehlers, K., and Kollmann, R. (2001). Primary and secondary plas-

modesmata: Structure, origin, and functioning. Protoplasma **216,** 1–30.

Gaire, F., Schmitt, C., Stussi-Garaud, C., Pinck, L., and Ritzenthaler, C. (1999). Protein 2A of grapevine fanleaf nepovirus is implicated in RNA2 replication and colocalizes to the replication site. Virology **264,** 25–36.

Geelen, D., and Inze, D. (2001). A bright future for the Bright Yellow-2 cell culture. Plant Physiol. **127,** 1375–1379.

Geldner, N., Friml, J., Stierhof, Y., Jurgens, G., and Palme, K. (2001). Auxin transport inhibitors block PIN1 cycling and vesicle trafficking. Nature **413,** 425–428.

Gillespie, T., Boevink, P., Haupt, S., Roberts, A., Toth, R., Valentine, T., Chapman, S., and Oparka, K. (2002). Functional analysis of a DNA-shuffled movement protein reveals that microtubules are dispensable for the cell-to-cell movement of *Tobacco mosaic virus*. Plant Cell **14,** 1207–1222.

Hecht, K. (1912). Studien über den Vorgang der Plasmolyse. Beitr. Biol. Pflanz. **11,** 133–145.

Heese, M., Mayer, U., and Jurgens, G. (1998). Cytokinesis in flowering plants: Cellular process and developmental integration. Curr. Opin. Plant Biol. **1,** 486–491.

Heinlein, M. (2002). The spread of tobacco mosaic virus infection: Insights into the cellular mechanism of RNA transport. Cell. Mol. Life Sci. **59,** 58–82.

Heinlein, M., Epel, B., Padgett, H., and Beachy, R. (1995). Interaction of tobamovirus movement proteins with the plant cytoskeleton. Science **270,** 1983–1985.

Heinlein, M., Padgett, H., Gens, J., Pickard, B., Casper, S., Epel, B., and Beachy, R. (1998). Changing patterns of localization of the tobacco mosaic virus movement protein and replicase to the endoplasmic reticulum and microtubules during infection. Plant Cell **10,** 1107–1120.

Holstein, S. (2002). Clathrin and plant endocytosis. Traffic **3,** 614–620.

Huang, M., Jongejan, L., Zheng, H., Zhang, L., and Bol, J. (2001). Intracellular localization and movement phenotypes of *Alfalfa mosaic virus* movement protein mutants. Mol. Plant-Microbe Interact. **14,** 1063–1074.

Huang, M., and Zhang, L. (1999). Association of the movement protein of *Alfalfa mosaic virus* with the endoplasmic reticulum and its trafficking in epidermal cells of onion bulb scales. Mol. Plant-Microbe Interact. **12,** 680–690.

Huang, Z., Han, Y., and Howell, S. (2000). Formation of surface tubules and fluorescent foci in *Arabidopsis thaliana* protoplasts expressing a fusion between the green fluorescent protein and the cauliflower mosaic virus movement protein. Virology **271,** 58–64.

Hugdahl, J., and Morejohn, L. (1993). Rapid and reversible high-affinity binding of the dinitroaniline herbicide oryzalin to tubulin from *Zea mays* L. Plant Physiol. **102,** 725–740.

Kasteel, D., Perbal, M., Boyer, J., Wellink, J., Goldbach, R., Maule, A., and van Lent, J. (1996). The movement proteins of cowpea mosaic virus and cauliflower mosaic virus induce tubular structures in plant and insect cells. J. Gen. Virol. **77,** 2857–2864.

Kasteel, D., van der Wel, N., Jansen, K., Goldbach, R., and van Lent, J. (1997a). Tubule-forming capacity of the movement proteins of alfalfa mosaic virus and brome mosaic virus. J. Gen. Virol. **78,** 2089–2093.

Kasteel, D., Wellink, J., Goldbach, R., and van Lent, J. (1997b). Isolation and characterization of tubular structures of cowpea mosaic virus. J. Gen. Virol. **78,** 3167–3170.

Lauber, M., Waizenegge, I., Steinmann, T., Schwarz, H., Mayer, U., Hwang, I., Lukowitz, W., and Jürgens, G. (1997). The Arabidopsis KNOLLE protein is a cytokinesis-specific syntaxin. J. Cell Biol. **139,** 1485–1493.

Lazarowitz, S., and Beachy, R. (1999). Viral movement proteins as probes for intracellular and intercellular trafficking in plants. Plant Cell **11,** 535–548.

Lin, B., and Heaton, L. (2001). An *Arabidopsis thaliana* protein interacts with a movement protein of *Turnip crinkle virus* in yeast cells and in vitro. J. Gen. Virol. **82,** 1245–1251.

Lukowitz, W., Mayer, U., and Jurgens, G. (1996). Cytokinesis in the Arabidopsis embryo involves the syntaxin-related KNOLLE gene product. Cell **84,** 61–71.

Maezawa, S., Yoshimura, T., Hong, K., Duzgunes, N., and Papahadjopoulos, D. (1989). Mechanism of protein-induced membrane fusion: Fusion of phospholipid vesicles by clathrin associated with its membrane binding and conformational change. Biochemistry **28,** 1422–1428.

Margis, R., Ritzenthaler, C., Reinbolt, J., Pinck, M., and Pinck, L. (1993). Genome organization of grapevine fanleaf nepovirus RNA2 deduced from the 122K polyprotein P2 in vitro cleavage products. J. Gen. Virol. **74,** 1919–1926.

Marks, M., Hiroshi, H., Kirshhausen, T., and Bonifacino, J. (1997). Protein sorting by tyrosine-based signals: Adapting to the Ys and wherefores. Trends Cell Biol. **7,** 124–128.

Mas, P., and Beachy, R. (1999). Replication of tobacco mosaic virus on endoplasmic reticulum and role of the cytoskeleton and virus movement protein in intracellular distribution of viral RNA. J. Cell Biol. **147,** 945–958.

McLean, B., Hempel, F., and Zambryski, P. (1997). Plant intercellular communication via plasmodesmata. Plant Cell **9,** 1043–1054.

McLean, B., Zupan, J., and Zambryski, P. (1995). Tobacco mosaic virus movement protein associates with the cytoskeleton in tobacco cells. Plant Cell **7,** 2101–2114.

Mellman, I. (1996). Endocytosis and molecular sorting. Annu. Rev. Cell Dev. Biol. **12,** 575–625.

Morejohn, L., Bureau, T., Molé-Bajer, J., Bajer, A., and Fosket, D. (1987). Oryzalin, a dinitroaniline herbicide, binds to plant tubulin and inhibits microtubule polymerization *in vitro*. Planta **172,** 252–264.

Morton, W.M., Ayscough, K.R., and McLaughlin, P.J. (2000). Latrunculin alters the actin-monomer subunit interface to prevent polymerization. Nat. Cell Biol. **2,** 376–378.

Nagata, T., Nemoto, Y., and Hasezawa, S. (1992). Tobacco BY-2 cell line as the "HeLa" cell in the cell biology of higher plants. Int. Rev. Cytol. **132,** 1–30.

Napier, R., Trueman, S., Henderson, J., Boyce, J., Hawes, C., Fricker, M., and Venis, M. (1995). Purification, sequencing and functions of calreticulin from maize. J. Exp. Bot. **46,** 1603–1613.

Nebenführ, A., Ritzenthaler, C., and Robinson, D. (2002). Brefeldin A: Deciphering an enigmatic inhibitor of secretion. Plant Physiol. **130,** 1102–1108.

Oparka, K., Prior, D., and Crawford, J. (1994). Behaviour of plasma membrane, cortical ER and plasmodesmata during plasmolysis of onion epidermal cells. Plant Cell Environ. **17,** 163–171.

Pont-Lezica, R., McNally, J., and Pickard, B. (1993). Wall-to-membrane linkers in onion epidermis: Some hypotheses. Plant Cell Environ. **16,** 111–123.

Pouwels, J., van der Krogt, G., van Lent, J., Bisseling, T., and Wellink, J. (2002). The cytoskeleton and the secretory pathway are not involved in targeting the cowpea mosaic virus movement protein to the cell periphery. Virology **297,** 48–56.

Reichel, C., and Beachy, R. (2000). Degradation of tobacco mosaic virus movement protein by the 26S proteasome. J. Virol. **74,** 3330–3337.

Remeta, D., Krumbiegel, M., Minetti, C., Puri, A., Ginsburg, A., and Blumenthal, R. (2002). Acid-induced changes in thermal stability and fusion activity of influenza hemagglutinin. Biochemistry **41,** 2044–2054.

Ritzenthaler, C., Laporte, C., Gaire, F., Dunoyer, P., Schmitt, C., Duval,

S., Piéquet, A., Loudes, A.M., Rohfritsch, O., Stussi-Garaud, C., and Pfeiffer, P. (2002a). Grapevine fanleaf virus replication occurs on endoplasmic reticulum-derived membranes. J. Virol. **76,** 8808–8819.

Ritzenthaler, C., Nebenführ, A., Movafeghi, A., Stussi-Garaud, C., Behnia, L., Pimpl, P., Staehelin, L., and Robinson, D. (2002b). Reevaluation of the effects of brefeldin A on plant cells using tobacco Bright Yellow 2 cells expressing Golgi-targeted green fluorescent protein and COPI antisera. Plant Cell **14,** 237–261.

Ritzenthaler, C., Pinck, M., and Pinck, L. (1995a). Grapevine fanleaf nepovirus P38 putative movement protein is not transiently expressed and is a stable final maturation product in vivo. J. Gen. Virol. **76,** 907–915.

Ritzenthaler, C., Schmit, A.-C., Michler, P., Stussi-Garaud, C., and Pinck, L. (1995b). Grapevine fanleaf nepovirus putative movement protein is involved in tubule formation in vivo. Mol. Plant-Microbe Interact. **8,** 379–387.

Roux, A., Cappello, G., Cartaud, J., Prost, J., Goud, B., and Bassereau, P. (2002). A minimal system allowing tubulation with molecular motors pulling on giant liposomes. Proc. Natl. Acad. Sci. USA **99,** 5394–5399.

Sambrook, J., Fritsch, E.F., and Maniatis, T. (1989). Molecular Cloning: A Laboratory Manual, 2nd ed. (Cold Spring Harbor, NY: Cold Spring Harbor Laboratory Press).

Samuels, A., and Staehelin, L. (1996). Caffeine inhibits cell plate formation by disrupting membrane reorganization just after the vesicle fusion step. Protoplasma **195,** 144–155.

Sanchez-Ferrer, A., Bru, R., and Garcia-Carmona, F. (1994). Phase separation of biomolecules in polyoxyethylene glycol nonionic detergents. Crit. Rev. Biochem. Mol. Biol. **29,** 275–313.

Sánchez-Navarro, J., and Bol, J. (2001). Role of the *Alfalfa mosaic virus* movement protein and coat protein in virus transport. Mol. Plant-Microbe Interact. **14,** 1051–1062.

Simons, K., and Ikonen, E. (1997). Functional rafts in cell membranes. Nature **387,** 569–572.

Staehelin, L., and Hepler, P. (1996). Cytokinesis in higher plants. Cell **84,** 821–824.

Steinborn, K., et al. (2002). The Arabidopsis PILZ group genes encode tubulin-folding cofactor orthologs required for cell division but not cell growth. Genes Dev. **16,** 959–971.

Storms, M., Kormelink, R., Peters, D., Van Lent, J., and Goldbach, R. (1995). The nonstructural NSm protein of tomato spotted wilt virus induces tubular structures in plant and insect cells. Virology **214,** 485–493.

Tang, B., and Hong, W. (1999). A possible role of di-leucine-based motifs in targeting and sorting of the syntaxin family of proteins. FEBS Lett. **446,** 211–212.

Thompson, G.A., Jr., and Okuyama, H. (2000). Lipid-linked proteins of plants. Prog. Lipid Res. **39,** 19–39.

Valster, A., and Hepler, P. (1997). Caffeine inhibition of cytokinesis: Effects on the phragmoplast cytoskeleton in living *Tradescantia* stamen hair cells. Protoplasma **196,** 155–166.

Verma, D. (2001). Cytokinesis and building of the cell plate in plants. Annu. Rev. Plant Physiol. Plant Mol. Biol. **52,** 751–784.

Völker, A., Stierhof, Y., and Jürgens, G. (2001). Cell cycle-independent expression of the Arabidopsis cytokinesis-specific syntaxin KNOLLE results in mistargeting to the plasma membrane and is not sufficient for cytokinesis. J. Cell Sci. **114,** 3001–3012.

Waigmann, E., Chen, M., Bachmaier, R., Ghoshroy, S., and Citovsky, V. (2000). Regulation of plasmodesmal transport by phosphorylation of tobacco mosaic virus cell-to-cell movement protein. EMBO J. **19,** 4875–4884.

Walker, F., deBlaquiere, J., and Burgess, A. (1993). Translocation of pp60c-src from the plasma membrane to the cytosol after stimulation by platelet-derived growth factor. J. Biol. Chem. **268,** 19552–19558.

Walkey, D., and Webb, M. (1968). Virus in plant apical meristems. J. Gen. Virol. **3,** 311–313.

Weerdenburg, C., Falconer, M., Setterfield, G., and Seagull, R. (1986). Effects of taxol on microtubule arrays in cultured higher plant cells. Cell Motil. Cytoskeleton **6,** 469–478.

Wellink, J., van Lent, J., Verver, J., Sijen, T., Goldbach, R., and van Kammen, A. (1993). The cowpea mosaic virus mRNA-encoded 48-kilodalton protein is responsible for induction of tubular structures in protoplasts. J. Virol. **67,** 3660–3664.

Wu, Y., He, Y., Bai, J., Ji, S.-R., Tucker, W., Chapman, E., and Sui, S.-F. (2003). Visualization of synaptotagmin I oligomers assembled onto lipid monolayers. Proc. Natl. Acad. Sci. USA **100,** 2082–2087.

Yasuhara, H., Sonobe, S., and Shibaoka, H. (1993). Effects of taxol on the development of the cell plate and of phragmoplast in tobacco BY-2 cells. Plant Cell Physiol. **34,** 21–29.

Ziegler, W., Tigges, U., Zieseniss, A., and Jockusch, B. (2002). A lipid-regulated docking site on vinculin for protein kinase C. J. Biol. Chem. **277,** 7396–7404.

Zuo, J., Niu, Q., Nishizawa, N., Wu, Y., Kost, B., and Chua, N. (2000). KORRIGAN, an Arabidopsis endo-1,4-β-glucanase, localizes to the cell plate by polarized targeting and is essential for cytokinesis. Plant Cell **12,** 1137–1152.